Università Politecnica delle Marche

PhD School in Human Health

The impact of Sleep Deprivation in the brain:
Endoplasmic Reticulum Stress and Myelin modification

Ph.D. Dissertation of:

Amina Aboufares El Alaoui

Tutor:

Prof. Simona Lattanzi

Curriculum supervisor:

Università Politecnica delle Marche

Department of Experimental and Clinical Medicine

Via Tronto 10A - 60126 - Torrette di Ancona, Italy

CONTENTS

ABSTRACT

Sleep deprivation (SD) is a huge problem for modern society. Clinical and preclinical studies have shown that SD is capable of inducing molecular, physiological, and biochemical changes at the central nervous system level. Previous molecular work has shown that sleep deprivation leads to endoplasmic reticulum (ER) stress in neurons, with a number of ER-specific proteins upregulated to maintain optimal cellular proteostasis. Furthermore, using electron and confocal microscopy, it has recently been shown that prolonged sleep restriction (~ 5 days) reduces myelin thickness and increases Ranvier node length without affecting internodal length, thus suggesting that sleep loss can lead to plastic remodelling of myelin. Through a multidisciplinary approach we have better explored the changes that SD induces in the ER network and at remodelling myelin.

Here we have verified that SD promotes changes in the ER network. Frontal cortex (layer II-III) neurons from dormant (S, n = 4, 127 neurons) and sleepless 6 hours (SD, n = 4, 132 neurons) mice were analysed with electron microscopy. It was found that in SD mice, the contacts between ER and mitochondria (mitochondria associated with membranes, MAM) were more numerous, that mitochondria tend to form clusters and the shape of the ER is more compact. The contacts between ER and plasma membrane (MAP) did not change. Interestingly, transcriptomic analysis of a previous gene expression database (GSE48369, Bellesi et al. 2013) revealed that vdac1, a key transcript of MAMs was upregulated after SD. Furthermore, it was evaluated whether SD is able to influence the fluidity of the myelin membrane through the use of steady-state fluorescence spectroscopy. In particular, two fluorophores were used, 2-dimethylamino- (lauroyl) -naphthalene (Laurdan), located at the hydrophobic-hydrophilic interface of the membrane and 1,6 diphenyl-1,3,5-hexatriene, incorporated in the hydrophobic lipid region. A significant increase in membrane fluidity was found in myelin membrane core in SD relative to S (DPH anisotropy: S [0.231 ± 0.008]; SD [0.222 ± 0.005], $p < 0.00019$), while no differences have been detected at the polar headgroups level. Thus, increased fluidity of the inner myelin membrane region could contribute to morphological modifications of myelin induced by sleep loss.

Additionally, using the same micrographs used for the ER network, a visual inspection of hundreds of manually segmented PAPs around the excitatory synapses of the somatosensory and cingulate cortex was performed. Several distinct organelles within PAPs were detected,

including empty and filled endosomes, phagosomes, mitochondria, and endoplasmic reticulum cisternae, distributed within three categories of PAP (branches, twigs, and leaflets). Most PAPs belonged to the leaflet category (~ 60%), with twigs representing a minority (~ 37%). The branches were rarely in contact with the synapses (<3%). Branches had a higher density of mitochondria and cisterns than ER at twigs and leaflets. Also, branches and twigs showed organelles more frequent than leaflets. Endosomes and phagosomes, which accounted for over 60% of all detected organelles, were often associated with the same PAP. Likewise, mitochondria and ER cisterns, which account for approximately 40% of all organelles, were associated with them. No differences were noted between the distribution of organelles in the somatosensory cortex and the anterior cingulate cortex. Finally, the distribution of organelles in PAPs did not depend on the presence of a spinal apparatus or presynaptic mitochondrion in the synapse enveloping PAPs, with some exceptions regarding the presence of phagosomes and ER cisterns, slightly more represented around synapses. lacking respectively a spinal apparatus and a presynaptic mitochondrion. Therefore, PAPs contain several subcellular organs that could underlie the different astrocytic functions performed centrally.

2. INTRODUCTION

Sleep Deprivation (SD) is caused by consistent lack of sleep or reduced quality of sleep Experiments of SD in animals have clearly shown that sleep is required for survival (Rechtschaffen and Bergmann 2002). However, the function of sleep remains elusive and there are still fundamental questions unanswered. It is well known that sleep plays an important role in learning, memory, mood, and judgment. (Institute of Medicine Committee on Sleep and Research, 2006). It is not surprising that negative public health consequences of sleep deprivation can be enormous. Some of the most devastating human and environmental disasters have been partially attributed to fatigue-related performance failures, sleep loss, and night shift work-related performance failures (Aserinsky and Kleitman, 1953). In addition, sleep loss has a significant economic impact at different level. Billions of dollars a year are spent on direct medical costs associated with doctor visits, hospital services, prescriptions, and over-the-counter medications for sleep-related problems. (Durmer and Dinges, 2005). Compared to healthy individuals, subjects with chronic sleep loss are less productive, have health care needs greater than the norm, and have an increased likelihood of injury (Killgore, 2010); this also represents an economic burden for society. Beyond that, the cumulative long-term effects of sleep loss have been associated with a wide range of deleterious health consequences, including an increased risk of hypertension, diabetes, obesity, heart attack, and stroke (Palagin et al., 2013, Tobaldini et al., 2017, Shigiyama et al., 2018). Over time, accumulating evidence has confirmed that sleep is essential for brain energy conservation (Tobaldini et al. 2017), brain waste clearance, modulation of immune responses (Besedovsky et al. 2019) and synaptic homeostasis (Tononi and Cirelli, 2000; Bellesi et al., 2017). It has also been demonstrated that SD leads to progressive physiological, biochemical, and molecular changes in the brain

(Rechtschaffen 1998; Pace-Schott and Hobson, 2002, Krueger 2008) . A crucial point in the study of SD is to clarify the extent to which these changes can affect human health and whether chronic sleep deprivation can induce deleterious and irreversible consequences.

2.2 ENDOPLASMIC RETICULUM STRESS AND SLEEP DEPRIVATION

One key aspect in cell biology relates SD to neuronal endoplasmic reticulum (ER) stress, even though little is known about the mechanisms linking these two phenomena. (Brown et al., 2014). Indeed, while the molecular mechanisms involved in ER stress are relatively well characterized, the metabolic events of ER stress that occur as a consequence of sleep deprivation and how they progress in this context remain largely undefined (Schröder ,2008). Recent evidence has shown that some genes altered by sleep deprivation are involved in protein biosynthesis, their transport and in the increase of oxidative stress (Ramanathan et al., 2002). One hypothesis is that ER stress is an attempt to cope with the increase in energy expenditure and metabolic changes that appears to occur during sleep deprivation (Sharma and Kavuru, 2010). Accumulating evidence demonstrates that where ER stress cannot be reversed, cellular functions deteriorate, often leading to cell death and contributing to the onset of many diseases (Sano and Reed, 2013). However, cellular death does not seem to happen in the case of sleep deprivation-induced ER stress: brains of rats exposed to prolonged sleep deprivation showed no obvious lesions. In particular a study showed that there was no increase in apoptosis or other neural markers of degeneration when examining 6-10 sections throughout the brain for all cell types after sleep deprivation (Cirelli et al. 1999).

The early stages of ER stress trigger an increase in mitochondrial metabolism that is critically dependent on organelle coupling and Ca^{2+} transfer to restore homeostasis. Within the ER network, the contact sites with the mitochondria and the plasma membrane, mitochondria associated membrane (MAMs) and plasma membrane associated membranes (PAMs),

respectively, play a particularly important role in maintaining cellular homeostasis. The onset of ER stress is also characterized by a redistribution of the ER network, particularly some groups showed that, during the early stages of ER stress, the interactions between the mitochondrial and reticular networks increase in number. Therefore, Ca^{2+} transfer to mitochondria is facilitated, thereby enhancing mitochondrial respiration (Bravo et al., 2011; Wang et al., 2011). Several studies have shown that these mechanisms seem to be a compensatory response undertaken to maintain the homeostasis of energy metabolism and to restore the functionality of proteins disrupted (Scharf, Naidoo et al. 2008) (Bravo, Gutierrez et al. 2012); this can be also the case when dealing with consequences of sleep deprivation. The idea that the subcellular and genetics consequences of sleep deprivation are triggered by metabolically driven changes induced by ER stress finds confirmation in various studies (Krueger, Rector et al. 2008). Several microarray studies have found that SD causes the overexpression of genes that encode proteins involved in the endoplasmic reticulum unfolded protein response (ER-UPR) as well as the mitochondrial unfolded protein response (MT-UPR) in the brain cortex (Naidoo, Giang et al. 2005; Chandra, Choy et al. 2007; Porter, Bohannon et al. 2012) . Using transcriptome analyses (mostly cDNA microarrays), more than ten research teams have compared the brains of rats, mice, sparrows, and flies in awake animals compared to asleep. The results of those studies suggest that sleep and wakefulness have particularly impactful effects on cellular processes related to energy metabolism, synaptic potentiation, and responses to cellular stress (Cirelli 2006) (Mackiewicz, Zimmerman et al. 2009). In a recent study, quantitative proteomics technologies performed to examine changes in the proteome of the entire mouse brain following sleep deprivation found that sleep deprivation had the strongest effect on the abundance of proteins related to mitochondrial stress responses and energy metabolism. (Gutierrez et al. 2012). On the other hand, it is known that the increase in mitochondrial metabolism is critically dependent on the coupling of organelles and on the

transfer of Ca^{2+}, and numerous ultrastructural studies associate the adaptive phase of ER stress with the increase of contact sites among the organelles that make up the network (De Stefani et al. 2009). However how and if SD induces this functional and structural adaptation of ER is still unclear.

2.3 SLEEP DEPRIVATION AND MYELIN

Recently, different studies indicated that sleep is also important for cell membrane and myelin maintenance in the brain and that these structures are particularly susceptible to insufficient sleep (Norbom et al. 2015). Moreover, some studies have shown that the genes involved in maintaining the plasma membranes of the cell are preferably transcribed during sleep suggesting that perhaps one of the functions of sleep may be to keep plasma membranes healthy (Bellesi et al. 2019). Many of these plasma membrane-related genes were found to be specific for myelin and were specifically upregulated over the course of several hours of sleep; in particular those genes coding for myelin structural proteins (Bellesi et al. 2019). The role of sleep in myelin maintenance are also confirmed by the downregulation of some myelin-related transcripts, both after acute (Hernandez et al. 2010) and chronic sleep deprivation (Cirelli et al. 2006); among these molecules, opalin, that is thought to be important for myelin stabilization at the paranodal site (Sato et al. 2008), and plasmolipin, that participates in the biogenesis of myelin by forming membrane domains at the Golgi level (Hugger et al. 2015). Studies confirmed that sleep can influence the proliferation of oligodendrocytes cells responsible to produce myelin. It has been found that hundreds of transcripts being translated in oligodendrocytes are differentially expressed in sleep and wake: genes involved in phospholipid synthesis and myelination or promoting oligodendrocyte precursor cells (OPC) proliferation are transcribed preferentially during sleep (Dgat2, Cds1, Elovl7, Chka, Opalin, Qk, Pllp, Sema4b, Sema6a, Tmod1, Slitrk6, Yap1, Nrg2, Rbn3, Mxd3, and Hydin); genes

implicated in apoptosis, cellular stress response, and OPC differentiation are enriched in wakefulness (Acin1, Bcat1, Otud7b, Nr4a1, Hip1, HSPE1, HSP90aa1, Irf8, and Traf6); sleep deprivation can alter this balance. Among these genes, it has been found the up regulation of Fad3 after sleep deprivation. This gene codes for a fatty acid desaturase that regulates the unsaturation of fatty acids and influences membrane fluidity (Bellesi et al.2019). It has also been found that in the cerebral cortex, the number of proliferating OPCs doubles during sleep compared to spontaneous wakefulness and sleep deprivation (Genskow et al. 2013). In addition to influencing the expression of genes and the oligodendrocytes proliferation, it has been found that structural changes in myelinated fibres are associated to acute and chronic sleep deprivation conditions. Bellesi and colleagues have shown that chronic sleep deprivation is associated with a thinner myelin sheath in two brain regions of adolescent mice (Haswell et al. 2018) compared to the sleeping mice. Consistently with this findings, studies in Humans indicate that sleep is important for cell membrane and myelin maintenance in the brain and that these structures might be particularly susceptible to insufficient sleep (Mikhail et al. 2012; Pfister-Genskow et al. 2013). A recent study, examining whether a waking day was associated with changes in brain imaging tensor diffusion parameters of healthy volunteers (Zhang et al. 2014), has shown that changes in white matter (WM) microstructure can occur within hours of awakening. Changes in WM functioning after one day of wakefulness and sleep deprivation have also been suggested by recent functional magnetic resonance imaging studies on connectivity (Tully et al. 2010; Westlye et al. 2018). Furthermore, another study observed diurnal changes in connectivity between regions of the medial temporal lobe and the cortex (Dosenbach et al. 2013), while others found that default mode network integrity was reduced after sleep deprivation (Tully et al. 2010; Parimal et al. 2012). Animal and human studies suggest that sleep deprivation can alter both the structure and function of myelin, however better investigation is needed.

3. AIM OF THE STUDY

The aim of this thesis is to better investigate the consequences of sleep deprivation at different levels. It is well known that sleep deprivation leads to endoplasmic reticulum stress in neuron with several ER-specific proteins being upregulated to maintain optimal cellular proteostasis. ER stress is also typically characterized by ER dynamic remodelling, which allows the formation of contact sites with other organelles and structures, including among others the mitochondria and the plasma membrane; however it is not clear if this reorganization of the ER network is also associated with sleep deprivation. Here we tested the hypothesis that SD promotes ER network modifications. We also used a genetically modified animal model of Drosophila with a higher number of MAMs to evaluate the effect that this modification of the ER network has in regulating sleep itself.

Furthermore, using the same method of analysis, we carried out a visual inspection of hundreds of manually segmented PAPs around excitatory synapses of the somatosensory and cingulate cortex, describing several distinct organelles within PAPs, which included empty and full endosomes, phagosomes, mitochondria, and endoplasmic reticulum cisternae.

Using electron and confocal microscopy it has been recently shown that prolonged sleep restriction (~ 5 days) reduced myelin thickness and increased node of Ranvier length without affecting internodal length, thus suggesting that sleep loss can lead to plastic remodelling of myelin (Haswell et al. 2018). Furthermore, it has been shown that SD induces the up regulation of Fad3 which regulates the unsaturation of fatty acids and influences their membrane fluidity. Since optimal fluidity of the plasma membrane is an essential requirement for cellular plasticity, we decided to evaluate whether the fluidity of membranes forming myelin could be affected by sleep loss.

4. MATERIALS AND METHODS:

4.1 Perysinaptic Astrocytic Processes and Endoplasmic Reticulum STRESS analysis

4.1.1 Tissue source and preparation

Male mice of four weeks of age C57BL6J were kept under a 12-h dark–light cycle (8AM-8PM) and permitted food and water ad libitum. Between 2-4PM mice were perfused intracardially under deep anaesthesia with a solution of 0.05 M phosphate buffered saline followed by 2.5 % glutaraldehyde and 4% paraformaldehyde in 0.1 M sodium cacodylate buffer (41 °C, pH 7.4). Brains were removed and kept in the same fixative overnight at 4 °C. Brain slices 300nm were cut on a vibratome and kept in a cryoprotectant solution until the day of processing. Sections were rinsed 3×10 min each in cacodylate buffer and incubated for 1 hr on ice with a solution of 1.5 % potassium ferrocyanide/2 % osmium tetroxide. After three rinses in double distilled water, they were exposed to a solution of 1 % thiocarbohydrazide for 20 min at room temperature. Sections were washed with distilled water and placed in 2 % osmium tetroxide for 30 min, washed again, and incubated overnight with 1 % uranyl acetate at 4 °C. The following day, the tissue was stained with a solution of lead aspartate, dehydrated, and embedded with Durcupan resin and ACLAR film. Small squares of tissue from anterior cingulate and somatosensory cortex (layer II-III) were glued on the tip of a metal pin and coated with silver paint to minimize specimen charging during imaging.

4.1.2 Image Acquisition and Analysis

Images were obtained using serial block-face electron microscope - ΣIGMA™ VP field emission scanning electron microscope (Carl Zeiss NTS Ltd) equipped with 3View® technology (Gatan Inc.), and a backscattered electron detector. Images were acquired using an

aperture of 30 μm, high vacuum, acceleration voltage of 1.2 kV, with image resolution (xy plane) between 4 and 6 nm. Serial images were obtained by scanning the face of an unsliced block of tissue placed inside the microscope, then cutting off ultrathin slices using an automated microtome within the instrument. The newly exposed surface of a sliced block was rescanned until a stack of images was obtained. The series of images were processed and analysed using FIJI. TrkEM2, a FIJI plug-in, from those images we carried out two different studies.

4.1.3 Endoplasmic Reticulum Ultrastructural analysis

4.1.3.1 Mitochondria Associated Membranes and Plasma Membrane Associated Membranes

From the micro-photograms obtained we analysed 123 neurons from layer II-III of the frontal cortex of sleeping animals and 117 neurons from layer II-III of the frontal cortex of the 6 hours-sleep-deprived animals. We first identified MAMs by measuring the distance between the ER and mitochondria, typically 10 to 20 nm. We then measured the length of the tracts in which the membranes of the two organelles run parallel to each other. Considering that each ER tubule can join the same mitochondrion in multiple contacts with some interruption, we measured multiple MAMs in the same mitochondrion. The same criteria were used to measure the length of the interactions between ER and PAMs.

4.1.3.2 Other structural changes in Endoplasmic Reticulum

In the same images, we also evaluated whether SD was able to induce other morphological modifications that normally occurs in response to ER stress, namely, changes of ER cisternae and mitochondria, in terms of shape and or size, and the formation of mitochondrial clusters. We analysed the images with the same software used for the identification of MAMs and MAPs, Image J FIJI. In all images we measured the area of each ER tubules and the area of the cytoplasm. Each cell was reconstructed from the micro-photograms to avoid repetitions.

4.1.4 Endoplasmic Reticulum Gene Analysis

From an analysis of the literature, we have identified a detailed catalogue of the ER and mitochondrial proteins. ER proteins were obtained from mouse brain by way of multidimensional separation techniques in combination with high-resolution tandem mass spectrometry (Stevens et al., 2008); mitochondrial proteins were obtained using in-depth tandem mass spectrometry (Calvo et al., 2016). From the forenamed ER proteins, we have extrapolated only the gene name relative to each ER protein, and from the MitoCarta2.0 we have pulled out only those genes belonging to the CNS with the aim of creating mouse brain ER (ER genes) and mitochondrial (Mito genes) gene lists.

Then we used the array data available at NCBI GEO database (GSE48369) to perform gene expression analysis of forebrain samples collected from sleeping (S; 6–7 h of sleep during the light phase) and sleep deprived (SD; 4 h of sleep deprivation through exposure to novel objects during the light phase) mice. Samples of this database were collected using the genetically targeted translating ribosome affinity purification (TRAP) methodology from bacterial artificial chromosome (BAC) transgenic mice expressing EGFP tagged ribosomal protein L10a in oligodendrocytes. BacTrap technique was used to isolate transcripts from oligodendrocytes (IP, the immunoprecipitated portion). However, the resulting non precipitated portion formed the unbound sample (UB) that was enriched in all the remaining cell types (neurons and other glia cells). RNA transcripts were extracted from both IP and UB samples of S and SD groups, but in the present study only array data obtained from the UB samples we used. Data were normalized within each behavioural state group using Robust Multiarray Average. To identify transcripts differentially expressed across S and SD, comparisons were carried out using the Welch's t test with Benjamini and Hochberg FDR

multiple-test correction. All genes with fold change > 30% and p < 0.01 were selected as S genes (if upregulated in S) and SD genes (if upregulated in SD) and used for subsequent analysis. To identify ER and Mito genes differentially expressed in S and SD, we intersected the ER and Mito genes with S and SD genes. Finally, transcriptional networks were created and analysed using STRING V10.5.

4.1.5 Western Blotting

Sleep (n=4) and SD (n=4) mice were dislocated and then decapitated; the whole brain was rapidly collected, dissected in cerebellum and forebrain, frozen on dry ice and maintained at −80°C for further use. Through a glass/glass tissue homogenizer, cerebellum and forebrain samples were homogenized in freezing homogenization buffer containing 10 mM HEPES, Sigma 1.0 mM EDTA, Promega 2.0 mM EGTA, Bioston BioProducts 0.5 mM DTT, Invitrogen 0.1 mM PMSF, Fluka Protease Inhibitor Cocktail, Roche 100 nM microcystin, Alexis. Next, 100 µL of each sample was boiled in 10 µL of Sodium Dodecyl Sulfate (SDS) at 90/95°C for 10 min and kept at −80°C.

Two Forebrain homogenate samples of each experimental group were pooled together. The protein concentration was evaluated with bicinchoninic acid assay (BCA assay). For both groups, cerebellum homogenate SDS samples (1µg/µL) and different concentrations (2µg/µL, 4µg/µL) of forebrain homogenate samples of each S and SD pool were resolved by Tris-HCl gel electrophoresis in 1X Tris/Glycine/SDS running buffer. Then, the proteins were transferred onto 0.45 µm pore size nitrocellulose membranes in 1X Tris/Glycine/Methanol transfer buffer. The membranes, in turn, were immunoblotted as follows: first, they were blocked in 5% non-fat dry milk in 1X PBS 0.1% Tween-20 with gentle shaking for 1h at room temperature; then, they were incubated for 2 h at room temperature with gentle shaking and overnight at 4°C with one of the following primary antibodies: anti-VDAC1 (Abcam #15895;

1:2000 in 1X PBS 0.1% Tween-20 with 0.5% non-fat dry milk); anti-STIM2 (Cell Signaling #4971; 1:1000 in 1X PBS 0.1% Tween-20).

The membranes were then rinsed 3 times in 1X PBS 0.1% Tween-20 and incubated with goat anti-rabbit secondary antibody (1:5000 in 1X PBS 0.1% Tween-20 with 3% non-fat dry milk) for 90 min at room temperature with mild oscillation. Blots were washed 3 times in 1X PBS 0.1% Tween-20 and finally with ddH_2O. Membranes were developed using an enhanced ECL Chemiluminescence Reagent (ECL-Prime, GE Healthcare) and the bands were revealed by exposition to Molecular Imager Chemidoc XRS+ (Bio-Rad). The optical density of the bands was quantified by ImageJ software (National Institutes of Health) and values were normalized to the average density of S samples.

4.1.6 Genetics and Drosophila strains

Fly stocks and crosses were maintained on standard cornmeal agar media at 25°C. The linker (a gift from Dr G. Csordás, Thomas Jefferson University, Philadelphia, USA), which encoded a monomeric red fluorescent protein (mRFP) preceded by the outer mitochondrial membrane targeting sequence mAKAP1 and followed by the ER targeting sequence yUBC6. This construct was codon optimised by site directed mutagenesis and cloned into the pUASTattB vector for PhiC31-mediated site-directed transgenesis. Transgenic flies were generated at the Cambridge fly facility (Department of Genetics, University of Cambridge, Cambridge, UK). The daGAL4, elav-GAL4 and UASmitoGFP were obtained from the Bloomington Stock Centre, UAS-Aβ42 arc was a kind gift from D. C. Crowther (Department of Genetics, University of Cambridge, Cambridge, UK), and UASmitycam was a gift from Professor Julian Dow (Institute of Molecular Cell & System Biology, University of Glasgow, Glasgow, UK).

We have cross-linked the Drosophila to obtain male linker flies and we have identified male mutant flies, visually distinguishable by the red eyes. All experiments on adult flies were

performed with males. Male progeny was harvested within 12 h after enclosure and kept in Drosophila activity monitor (DAM) glass tubes. Parents and progeny were cultured with standard cornmeal molasses and maintained and tested at 20 °C temperature, 68% humidity, on a 12 h:12 h light: dark cycle.

At the beginning of the experiment, single flies were placed in the DAM glass tubes with enough food for 1 week of recording. Monitors were housed inside environmental chambers where temperature and humidity were kept constant (20 °C, 68%). Data analysis was performed using custom-designed software developed in our laboratory. We monitored their behavioural state during the light and dark phase

4.1.7 Characterization of Subcellular Organelles in Cortical Perisynaptic Astrocytes

In the images serially collected we identified the axo-spinous asymmetric (excitatory) synapses in the neuropil. For each synapse, we defined the Axon-Spine Interface (ASI) as the interfacing surface between the spine and the axonal bouton, and a cuboid region of interested (ROI) was drawn around the synapse. ROI included the axon terminal, the post-synaptic element, and the peri-synaptic astrocyte (PAP) when present. PAPs were recognized from their distinctive shapes, interdigitating among neuronal profiles often contacting parts of the synapse, and from the presence of glycogen granules. Other elements of the neuropil such as cell bodies, blood vessels, or large dendrites were not included in the ROI. For each ROI, two blinded scorers segmented the spine head, the ASI, the PAPs, and identified all the organelles included in the PAP. Five different types of organelles were recognizable: 1) empty endosomes (EE), described as vesicular structures with a diameter of 80-150 nm often showing a clear endoplasm with no inclusions; 2) full endosomes (FE) described as endosomes containing smaller vesicles or amorphic material; 3) Phagosomes (PH) described by the presence of a portion of axon, spine head, or dendrite being invaginated by the surrounding PAP, with a clear

continuity between the part being enclosed by the PAP (phagosome) and the neuronal structure; 4) Mitochondria; 5) ER cisternae described as long tubular structures. We also estimated the number of synapses contacted by PAP at post-synaptic site (Spine + synapses) or at cleft level (ASI + synapses) and the extent of synaptic coverage quantified as the interfacing apposed surface between the PAP and the post-synaptic element. To estimate whether organelles are isolated or tend to group together, we performed a cluster analysis by correlating the occurrence frequency within the same PAP of two or more organelles.

4.2 MYELIN ISOLATION

4.2.1 Tissue source and preparation

Mice from lineage C57BL/6 were housed in the same environmental condition in a number of 6 mice for cage with free access to food and water. The acute SD was carried out manually by the experimenter, by exposing animals for 6 hours to novel objects, and gentle handling them, paying attention to not cause any stress to them. All the mice were anesthetized with isoflurane and killed by cervical dislocation, in a time frame to collect all the brain within the same circadian window. Myelin enriched brain samples was obtained by using the protocol described by Larocca (Norton et al. 1974). The methods used to prepare myelin involve homogenization of the tissue in isotonic sucrose solution, followed by the isolation of myelin membranes by a series of steps that include density gradient centrifugation and differential centrifugation. The procedure was carried out by the same experimenter to be reproduced as faithfully as possible. The experiment was repeated four times in a total of 42 mice form S group and 38 from SD.

4.2.2 Steady-State fluorescence spectroscopy

Steady state fluorescence spectroscopy has been used to evaluate changes of myelin fluidity. The fluorescence measurements have been performed at 37°C with a computer-controlled

PerkinElmer LS55 spectrofluorometer. The temperature was measured in the sample by a digital thermometer. The background fluorescence of the samples was checked prior to each measurement and was negligible when the probes were added. Stock solutions of 6-dodecanoyl-2-dimethylamine-naphthalene (Laurdan) in ethanol and 1,6-diphenyl-1,3,5-hexatriene (DPH) in tetrahydrofuran were added to myelin samples at final probes concentration of 1 μM. Laurdan, locates at the hydrophobic-hydrophilic interface of the membrane; its spectral changes have been used to calculate the generalized polarization (GP), a function which gives information about the lipid packing related to the water content and dynamics at the lipid interface (Gratton et al. 1999). Laurdan excitation GP (Ex GP) and emission (Em GP) spectra have been calculated as follow (Loiero et al. 1993): Ex GP = $(I_{440}-I_{490})/(I_{440}+I_{490})$, where I_{440} and I_{490} are the intensities at each excitation wavelength, from 320 to 420 nm, obtained using a fixed emission wavelength of 440 and 490 nm, respectively;   Em GP = $(I_{390}-I_{360})/(I_{390}+I_{360})$, where I_{390} and I_{360} are the intensities at each emission wavelength, from 420 nm to 550 nm, obtained using a fixed excitation wavelength of 390 and 360 nm, respectively. DPH locates at the core level of the membrane and the steady-state fluorescence anisotropy, which gives information of lipid packing (Lentz 1989), was calculated by using the following equation: $r_s = (I_{||} - I_{\cdot} \, xg)/(I_{||} + 2I_{\cdot} \, xg)$ where g is an instrumental correction factor, $I_{||}$ and $I_{\cdot}$ are, respectively, the emission intensities with the polarizers parallel and perpendicular to the direction of the polarized exciting light.

5. RESULTS

5.1 GENE ANALYSIS

To identify the genes specific to ER and mitochondria differentially expressed in SD condition, we interrogated a gene dataset previously obtained in the context of a study aiming at detecting oligodendrocytes and other brain cells genes modulated by sleep and wake. In that study, we

used the array data relative to the 'other brain cells' that contain largely neurons and astrocytes. This transcriptional data set was obtained from the forebrain region of S mice (6–7 h of sleep during the light phase; n = 6), and SD mice (4 h of forced enriched wake during the light phase, n = 6). Using a FDR of 1%, we identified 2538 genes changing their expression because of S and SD. Of those, 1197 genes were upregulated during S and 1341 after SD. Then, we intersected S and SD gene lists with the mouse brain ER (ER genes containing 1899 unique genes) and mitochondrial (Mito genes containing 829 unique genes) gene lists to finally identify the ER and Mito genes differentially expressed in S and SD. The resulting Venn diagrams showed that 99 genes were mutually expressed in the ER and SD (ER-SD), while 71 genes belonged to both ER and S genes (ER-S). In addition, 29 genes were shared between mitochondria and SD (Mito-SD) and 18 genes were in common to mitochondria and S (Mito-S). Of note, we found that Hspa9, Vdac1 and Snd1 were amongst the highly significant ER and Mito genes overexpressed after SD, suggesting an important response of the ER and mitochondria to SD. These findings were confirmed by a transcriptional network analysis that revealed that both ER-SD and Mito-SD networks have significantly more interactions than chance (ER-SD: number of nodes: 99; number of edges: 132; average node degree: 2.67; average local clustering coefficient: 0.37, PPI enrichment p-value: 2.81e-12. Mito-SD: number of nodes: 29; number of edges: 22; average node degree: 1.52; average local clustering coefficient: 0.36, PPI enrichment p-value: 5.16e-08), with the most transcriptionally reshaped landscapes associated with ER stress and chaperone function, MAMs, and respiratory chain activity. By contrast, the ER-S transcriptional network analysis showed no significant clusters (number of nodes: 71; number of edges: 29; average node degree: 0.8; average local clustering coefficient: 0.44, PPI enrichment p-value: 0.09), while Mito-S analysis showed the formation of two significant clusters (number of nodes: 18; number of edges: 7; average node degree: 0.8;

average local clustering coefficient: 0.3, PPI enrichment p-value: 3.04e-05) relative to aminoacyl-tRNA biosynthesis and mitochondrial ribosomal subunit assembly

6.1 ENDOPLASMIC RETICULUM STRESS ANALYSIS

6.1.1 Ultrastructural studies

Transcriptomic analysis has revealed the ER and mitochondria strongly responded to SD with changes in the expression of genes involved in specific functions, such as ER stress, MAMs, and mitochondrial respiratory activity. To evaluate whether these SD dependent molecular effects were associated with ER and mitochondrial structural modifications, we analysed electron microphotographs of 123 and 117 neurons from frontal motor cortex obtained from S and SD mice, respectively. We focused on cell somas where there was abundance of ER cisternae and mitochondria.

We first identified the MAMs by measuring the distance between the ER and the mitochondria, typically less than 20 nm. Therefore, the length of the tracts in which the two membranes of the organelles run parallel to each other were measured **(Figure 1A).** Manual segmentation and analysis of ER and mitochondria showed that the normalised number of ER cisternae per cytoplasmic area was higher in SD than in S, but the overall area occupied by ER cisternae did not change (**Figure 1B**). Although the ER area was not affected by SD, ER bidimensional shape did. By estimating the ER compactness (i.e. a measure representing the degree to which a shape is compact) through dimension (perimeter/area ratio) and dimensionless (ratio area×(perimeter)-2) measures, we found that ER shape in SD was less convoluted and more rounded than in S. Regarding MAMs, we found that, although the average length of MAMs did not differ between S and SD, the number of MAMs, quantified as number per mitochondrion, was remarkably increased in SD (**Figure 1C**). Interestingly, a small portion of cells (<10 out of more than 100) showed very high values of MAMs density (up to two-three

times the values observed in S; **Figure 1D).** Thus, these data indicate that SD increases the number and shape of ER cisternae and promotes the formation of MAMs. While the analysis of the points of contacts between the ER and PAM, revealed that both PAMs length and number did not change between S and SD (**Figure 1E**). Finally, we assessed morphological changes in mitochondria by measuring the density of mitochondria and the cytoplasmic area occupied by them. Neither density nor mitochondrial area were affected by SD. However, when we considered the number of contacts between mitochondria, we found that SD was associated with a higher number of contacts, and with an increased capability of mitochondria of forming clusters (**Figure 1F**). Furthermore, by quantifying the number of contacts between mitochondria and plasma membrane, it was found that the occurrence was more frequent in SD, although it was overall very rare in both conditions.

6.1.2 Western blot result

To confirm this structural finding, we measured by western blotting the expression of the protein VDAC1 in brain homogenates of S and SD mice. VDAC1 is a protein participating in the formation of MAMs, whose mRNA transcript value was also significantly upregulated in SD. Semiquantitative analysis at western blotting confirmed that VDAC1 levels were higher in SD than in S condition.

6.1.3 Drosophila Sleep Deprivation experiment

Results so far have shown that SD promoted ER remodelling leading to the formation of new MAMs allowing the communication between ER and mitochondria. To understand whether increased MAMs were only a consequence of SD or, instead, they played some active role in regulating sleep, we took advantage of a Drosophila model, in which the formation of MAMs was forced by the overexpression of a synthetic linker between the mitochondria and the ER in brain neurons. Male mutant flies (n=181, elav > linker) and both parental controls (n=118,

elav/+, n=212, linker/+) were housed in monitor chambers for 3-4 consecutive days in order to a have a reliable measure of their sleep and wake activity (**Figure 2A-C**). Relative to both parental controls, linker-mutant flies slept less than both wild type controls (elav > linker vs elav/+: -11.5 ± 0.18%, p<0.001; elav > linker vs linker/+: -6.2 ± 0.09%, p<0.001). This decrease was particularly appreciated during the dark period (elav > linker vs elav/+: -18 ± 0.32%, p<0.001; elav > linker vs linker/+: -6.2 ± 0.11%, p<0.001), when flies are usually mostly asleep. The reduction in sleep time was accompanied by an overall increase of number of short duration sleep episodes (number: elav > linker vs elav/+: +22.6 ± 0.79%, p<0.001; elav > linker vs linker/+: +13.7 ± 0.38%, p=<0.001; duration: elav > linker vs elav/+ : -31.3 ± 1.64%, p<0.001; elav > linker vs linker/+: -18.5 ± 0.79%, p<0.001), culminating in a decreased sleep stability (elav > linker vs elav/+: -58 ± 7.85%, p<0.001; elav > linker vs linker/+: -38.3 ± 5.18%, p=0.001). Sleep latency did not differ among groups (elav > linker vs elav/+: p=0.27; elav > linker vs linker/+: p=0.99).

Thus, enhancing the formation of MAMs in brain neurons of flies is associated with shorter and less consolidated sleep.

7.1 MYELIN FLUIDITY ANALYSIS

As mentioned before, previous analysis of the oligodendroglia transcriptome revealed the up regulation of Fad3 in SD (+176%; p=0.004). Fad3 codes for a fatty acid desaturase that regulates unsaturation of fatty acids and influences membrane fluidity. Since optimal plasma membrane fluidity is an essential requirement for cellular plasticity, we hypothesized that the fluidity of membranes forming myelin could be affected by sleep loss. A significant increase in membrane fluidity was found in myelin membrane core in SD relative to S (DPH anisotropy: S [0.231±0.008]; SD [0.222±0.005], p<0.00019), while no differences have been detected at the polar headgroups level (**Figure 3A-B**).

Thus, increased fluidity of the inner myelin membrane region could contribute to morphological modifications of myelin induced by sleep loss.

8.1 PERISYNAPTIC ASTROCYTIC PROCESS ANALYSIS

8.1.1 Perisynaptic Astrocytic Process Surrounding Axo-Spinous Synapses

To characterize the subcellular composition of PAPs in relation to axo-spinous synapses, we analysed two different brain regions, the somatosensory (SSC) and the anterior cingulate (ACC) cortex of adolescent mice (n = 4). We hypothesized that since these two cortical regions are involved in different brain functions and belong to a different hierarchical order, they would also have a heterogenous organelle composition within PAPs. By following astrocytic profiles in three dimensions, PAPs surrounding axo-spinous synapses were easily identified: they often displayed sharp angles, contained glycogen granules, and interdigitated between neuronal structures. For each synapse, we reconstructed the pre-and post-synaptic elements and the PAPs within a three-dimensional ROI. In the two cortical regions, we sampled a comparable volume of neuropil (ROI volume in ACC: 0.66 ± 0.16 μm^3; in SSC: 0.48 ± 0.09 μm^3; p = 0.09), PAP volume (in ACC: 0.06 ± 0.01 μm^3; in SSC: 0.05 ± 0.01 μm^3; p = 0.07), ratio between PAP and ROI volume (ACC: 0.1 ± 0.01, SSC: 0.1 ± 0.02; p = 0.7; **Figures 4A–D**), and synapses of similar size, as shown by the distribution of ASI measures (ACC: 0.18 ± 0.03 μm^2; SSC: 0.19 ± 0.03 μm^2; p = 0.6; **Figure 4E**).We found that the fraction of synapses contacted by a PAP at the post-synaptic site was $78.6 \pm 6.3\%$ in ACC and $79.4 \pm 2.1\%$ in SSC (p = 0.8); the fraction of synapses contacted by PAP at the synaptic cleft was $50.39 \pm 1.27\%$ in ACC and $53.79 \pm 3.09\%$ in SSC (p = 0.1; **Figure 4F**). Synapses not contacted by PAP represented $22.4 \pm 6.3\%$ in ACC and $21.6 \pm 2.1\%$ in SSC (p = 0.8; not shown). Finally, we found that the extent of PAP coverage around the post-synaptic element was comparable

between the two cortical regions (ACC: 0.14 ± 0.01 μm^2; SSC: 0.15 ± 0.04 μm^2; p = 0.65; **Figure 4G).**

8.1.2 Perysinaptic Associated Processes Contain Multiple Subcellular Organelles

Visual inspection of 863 manually segmented PAPs surrounding axo-spinous synapses of the SSC and ACC cortex identified 23 branches (2.66%), 323 branchlets (37.38%), and 517 leaflets (59.95%; **Figure 5A**). As expected, branches, branchlets, and leaflets displayed different values of surface to volume ratio, with leaflets having a more convoluted and less rounded shape than branchlets and branches (**Figure 5B**). We detected five classes of subcellular organelles in PAPs: EE, FE, PH, MT and ER (see Materials and Methods; **Figures 6A–E**). We applied a mixed-effect model (REML) with cortical region and type of organelle as fixed factors to assess the organelle distributions in branches, branchlets, and leaflets. It was found that cortical region did not influence the distribution of these organelles within branches, branchlets, and leaflets (p = 0.13), but the density of ER and MT was significantly higher in branches relative to branchlets and leaflets (p < 0.0001; Figure **7A**). No significant differences were observed between leaflets and branchlets.

When evaluating the fraction of branches, branchlets, and leaflets containing at least one of the mentioned organelles, we found that leaflets had organelles in $8.54 \pm 5.02\%$ of the cases, branchlets in $32.49 \pm 13.5\%$, and branches in $47.22 \pm 21.8\%$. Leaflets contained organelles less frequently than branchlets, for all classes of organelles [REML with cortical region and type of organelle as fixed factors, effect found for type of organelles p < 0.0001; post hoc tests for EE (p = 0.046), FE (p = 0.022), PH (p = 0.02), MT (p = 0.022), ER (p = 0.016)], whereas the difference was significant only for MT (p = 0.01) and ER (p = 0.021) when leaflets were compared to branches. Among all organelles, mitochondria were the least present in leaflets.

When comparing branchlets and branches, we found that the fraction of branches containing MT was higher than the branchlets' one (p = 0.002; Table 1, **Figure 7B**). In PAPs, organelles can appear alone or be associated with each other within the same PAP. To test the likelihood of finding clusters of multiple organelles and identify which organelles tend to co-occur, we carried out a correlation matrix of the organelle distribution frequency. After correcting for multiple comparisons (Bonferroni), no clusters were found when branches, branchlets, and leaflets were considered independently (**Figure 8A**). However, when branches, branchlets, and leaflets data were pooled together to increase statistical power, three main clusters of organelles significantly co-occurring in PAPs were found: the first cluster linked together EE, FE, and PH, the second cluster linked EE and FE with ER, and the third ER and MT (**Figure 8B**).

8.1.3 The Presence of Mitochondrion and Spine Apparatus Influences the Distribution of Some Organelles of the Surrounding Perisynaptic Astrocytic Processes

Astrocytes usually tend to enwrap synapses with their PAPs often reaching the synaptic cleft. Thus, given the strong anatomical and functional interrelationship between neuronal and astrocytic structures, we hypothesized that the PAP's organelles may play a role in the modulation of synaptic function, and that differences in organelle composition inside the PAP may reflect different needs specific for different types of synapses. To test this hypothesis, we divided synapses based on the presence either of a spine apparatus in the postsynaptic compartment or of a mitochondrion in the presynaptic element, and tested whether these different classes of synapses determined a different organelle distribution within the PAPs around them. Given the small number of astrocytic branches surrounding synapses, only branchlets and leaflets were considered for this analysis. Also, their data were pooled together,

as their organelle distributions were comparable. Repeated measure three-way ANOVA found a main effect of spine apparatus (F $(1,15)$ = 76.62; p < 0.0001) and presynaptic mitochondria (F $(1,15)$ = 34.30; p < 0.0001). Post hoc analysis revealed a significant effect for PH (p = 0.0226), which occurred more frequently in PAPs contacting synapses without spine apparatus, and for ER, which were more frequent in PAPs contacting synapses without a presynaptic mitochondrion (p = 0.0231). None of the other organelles showed a significant difference (**Figures 9A,B**).

8.2 DISCUSSION:

The present study was the first to show that the ER and mitochondria strongly respond to acute SD with changes in the expression of genes involved in specific functions, such as ER stress, MAMs, and mitochondrial respiratory activity. Furthermore, we confirmed that these SD dependent molecular effects were associated with an increase in MAMs number, the formation of mitochondrial clusters and modifications of ER cisternae. We also found an increased fluidity of the inner myelin membrane region as a consequence of acute sleep loss. Furthermore, our work was also the first to disprove the common belief that PAPs lack most intracellular organelles such as mitochondria, ER, with vesicles (endosomes) observed only occasionally.

9.1 Sleep deprivation and Endoplasmic Reticulum network

9.1.1 Gene analysis

Sleep deprivation can induce ER stress, a condition in which ER homeostasis is disrupted leading to accumulation of misfolded proteins. Under this condition, the ER puts in place a cytoprotective response called Unfolded Protein Response (UPR) to attempt to restore the ER proteostasis (Papa et al. 2015). In this study, we have found that the expression of some genes, localized specifically at MAMs, has a high significance in SD mice. As described above, MAMs are specialized sub compartments involved in different functions, namely transferring of Ca^{2+} from the ER to mitochondria, appropriate mitochondria bioenergetics and others. In addition, MAMs seem to have a role in the transfer of stress signals from ER to mitochondria (Vliet et al. 2017). Among the genes differentially expressed in SD, we can mention Hspa9 and Vdac1. The Hspa9 gene is located on chromosome 5q31.2 and encodes for one of the 70 family members heat shock protein, also known as GRP75 (glucose-regulated protein75). This protein functions as a molecular chaperone and regulates cellular stress response, cell proliferation and

apoptosis by interacting with other proteins (Liang et al. 2017). It has been found in mitochondria, endoplasmic reticulum, plasma membrane, though it is present in other subcellular compartments. GPR75 ties the N-terminal domain of the Inositol 1,4,5-trisphosphateReceptors (IP3R) to Voltage-dependent anion-selective channel 1 (VDAC1) creating a molecular bridge that increases the Ca^{2+} accumulation in mitochondria by stabilizing the coupling of the two receptors (Rossin et al. 2018). The IP3R-GRP75-VDAC complex is present at the MAMs, where it plays a crucial role in the regulation of the intracellular Ca^{2+} (Suski et al. 2011). The Vdac1 gene is located on the chromosome 5q31.1 and encodes for the protein VDAC1 which forms an ion channel in the outer mitochondrial membrane (OMM), where it regulates the crosstalk between mitochondria and the rest of the cell. Specifically, VDAC1 mediates both the Ca^{2+} transport from the ER to mitochondria at MAMs and the cellular energy production by transporting ATP/ADP, NAD+/NADH and acyl-CoA from the cytosol to the intermembrane space (IMS). Moreover, it is responsible for the metabolite and ion transport and takes part to the apoptosis (Nahon-Crystal et al. 2018). Protein folding is an energetically demanding process that requires ATP to guarantee chaperone function, Ca^{2+} homeostasis as well as ER redox. The accumulation of misfolded proteins in the ER stress requires an increased production of ATP to provide for an increased amount of ER chaperones. In this context, the augmented mitochondria calcium concentration triggers the activation of the oxidative phosphorylation system (OXPHOS) leading to increased ATP synthesis. Indeed, it has been demonstrated that an increased mitochondria calcium concentration is followed by increased NADH production in various cell types (Boneh, 2006). Two key mitochondrial metabolic enzymes (a-ketoglutarate and isocitrate dehydrogenase) are activated by Ca^{2+} through its direct binding to the enzyme complexes (Bianchi et al. 2004). These two enzymes play pivotal role in the citric acid cycle ensuring NADH production, which in turn is used in the OXPHOS to generate ATP. Another important gene whose expression is significant in both

organelles analysed in SD mice is the Snd1. This gene is located on the chromosome 7q32.1 and encodes for the protein Staphylococcal Nuclease Domain-containing protein 1 (SND1), a multidomain protein acting as a nuclease and ligand. SND1 regulates posttranscriptional processes linked to RNA splicing, editing, and silencing. SND1 plays an important role in RNA protection since it interacts with stress granules protein components and degrades highly mutated, hyper-edited regions of double stranded RNAs generated during the cellular stress response (Park et al. 2010). Armengol et al. (2014) have demonstrated that ER stress is an up-regulating factor for SND1 gene expression. It may be caused by the fact that if ER stress persists, a group of cellular mRNAs is translationally silenced by sequestration into discrete cytoplasmic stress granules until stress mitigates or degradation; thus, SND1 may take part in this process. Oxidative stress is able to determine stress granule formation (Zhang et al. 2016). Since ER stress contributes to the greater production of ROS due to the increment of OXPHOS, it could speculate that, as a consequence, this oxidative environment may also trigger a higher expression of Snd1 gene in mitochondria to let it interacts with stress granules. The gene Slc25a25, located on the chromosome 9q34.11 and encoding for the protein Calcium-binding mitochondrial carrier protein SCaMC-2 (SLC25A25), has a significant expression in mitochondria and SD. This protein is present in the inner membrane of mitochondria where it functions as shuttle for metabolites, nucleotides, and cofactors between the cytosol and mitochondria, and as ATP-Mg^{2+}/Pi carrier catalysing an electroneutral exchange of ATP-Mg^{2+} for Pi. The protein SLC25A25 is a member of the subgroup of short calcium-binding MC (SCaMCs) which have a bipartite structure: he C-terminal half is homologous with MC family members and the N-terminal extension carries EF-hand motifs. It has been hypothesized that in muscle SLC25A25 functions in controlling ATP and Ca^{2+} homeostasis by means of its structural properties and its high level of expression (Zhang et al. 2011). Due to its high significance in mitochondria and SD, we may presume that SLC25A25 could play a similar

role in the context of ER stress as condition determined by SD. An additional gene to mention, whose expression is particularly significant in the ER and SD, is Homer1. It is located on the chromosome 5q14.1 and encodes for the postsynaptic density scaffolding protein Homer protein homolog 1 (HOMER1). Homer family proteins share a conserved N-terminal Ena/VASP homology 1 (EVH1) domain which functions as a protein-protein interaction motif to bind a proline-rich consensus sequence in various other scaffolding and signal transduction molecules (Pouliquin et al. 2009). This family is composed of two major groups: the short-form protein of HOMER1A and the long-form proteins of HOMER1B/C, HOMER2, and HOMER3. The long Homer proteins have an additional coiled-coil structure in the carboxylic terminal regions, that leads them to form specific self-associations and couple group I metabotropic glutamate receptors (group I mGluRs), and Inositol 1,4,5-triphosphate receptors (IP3Rs) to form an efficient signaling complex (Peng et al. 2020). In fact, HOMER1 long-form proteins dimerize and interact with metabotropic glutamate receptors and IP3Rs increasing Ca^{2+} release from the ER pools in neuronal cells. Moreover, it has been shown that the expression of the gene Homer1a, which encodes for the short HOMER1 protein, is significantly augmented in mice with 6h of SD at the light onset (Dorsaz et al. 2007). The gene Ywhab located on the chromosome 20q13.12 encodes for the 14-3-3 protein beta/alpha (the α isoform is known as phosphorylated form β). The 14-3-3 proteins are a highly conserved family with a subunit mass of approximately 30 kDa, that play key roles in various cellular processes such as signal transduction, cell cycle control, stress responses, and malignant transformation; this is possible through their multiple interactions with various kinases, receptors, enzymes, and structural and cytoskeletal proteins, in a phosphorylation-dependent manner (Kawahara et al. 2006). Proteins 14-3-3 are abundant in brain tissue where are present within synapses, contributing to several cellular processes, for instance ion channel regulation and intracellular trafficking (Brennan et al. 2012). Further, these proteins can also function as sweepers of

misfolded proteins and promote protein trafficking from the endoplasmic reticulum (Lewis et al. 2002) (Hachiya et al. 2006).

9.1.3 Ultrastructural studies of Endoplasmic Reticulum network

Previous molecular work has shown that SD leads to ER stress in neurons, with several ER-specific proteins being upregulated to maintain optimal cellular proteostasis (Chan et al. 2014). Specifically, Naidoo and colleagues found that 6 hours of SD can induce ER stress in mice with increased expression of many molecules involved in Unfolded Protein Response and that their expression increases after 9 and 12 hours of SD (Bip protein, pPERK, pEIFα) (Naidoo et al. 2005). However, it remains unclear whether SD induced ER stress is associated with structural ER modifications or whether ER interaction with other cellular structures are promoted. Through our transcriptomic analysis, we took a step forward by demonstrating that acute SD induces changes in the expression of genes involved in specific functions, such as ER stress, MAMs, and mitochondrial respiratory activity. Therefore, we have shown that ER and mitochondria respond strongly to SD. Indeed, it is well known that metabolic abnormalities, occurring under ER stress, such as perturbation of calcium and lipid homeostasis, induce on one hand numerous alterations in mitochondrial behaviour and function, including reduced respiratory chain activity and oxidative phosphorylation, increased free radical production, and on the other hand altered organellar morphology, dynamics, and positioning (Schon, 2018). These modifications include enhanced interaction of the ER with mitochondria of the interaction of the ER and plasma membrane (Kozieł et al. 2009) and alteration of size and shape of ER itself (Schuck et al. 2009). ER stress is a key factor in numerous neurodegenerative diseases (Endres et al. 2013), diabetes (Vincent et al. 2013), obesity, chronic pain (Yousuf, et al. 2020). Accumulating evidence demonstrate that where ER stress cannot be reversed, cellular functions deteriorate, often leading to cell death (Sano et al. 2013). Although the mechanism

is far from being understood, one hypothesis is that ER stress is an attempt to cope with the increase in energy expenditure and metabolic changes that appears to occur during the pathophysiological mechanisms (Sano et al. 2013). Our ultrastructural analysis was coherent with the transcriptomic analysis and with the morphological modifications that usually occur during ER stress. We may presume that the increase of MAMs, the formation of the mitochondrial clusters, and the changes in the shape of ER cisternae could be a consequence of coping with the increase of mitochondrial bioenergetic demand that occurs during SD (Cirelli et al. 1998). In previous studies, Bellesi's group had already shown that prolonged wakefulness is capable of inducing structural changes in the brain. In detail, they showed that acute SD and chronic sleep loss increase the number of astrocyte-mediated phagocytic events in the mouse cortical neuropile, whereas only chronic sleep loss can trigger microglial phagocytosis (Bellesi et al. 2017). It has been hypothesized that increased brain metabolism, mitochondrial bioenergetic demand, free radical production, and increased lipid peroxidation as a consequence of prolonged wakefulness are the cause of these structural changes (Bellesi et al. 2017). Indeed, it has been demonstrated that brain metabolism is 15–20% higher in wake than in sleep, and that prolonged wake can increase protein synthesis with an upregulation of some genes involved in energy metabolism (type I glucose transporter Glut1, Vgf), in growth factors / adhesion molecules (BDNF, TrkB, adhesion molecule F3), and in chaperones / heat shock proteins (BiP, ERP72, GRP75, HSP60, HSP70) (Tononi et al. 2001) coupling and Ca^{2+} transfer in order to restore homeostasis (Buchanan et al. 2006). For example, we hypothesize that the early stages of SD-induced ER stress trigger an increase in mitochondrial metabolism critically dependent on organelle coupling and Ca^{2+} transfer in order to restore homeostasis. Although there are no direct studies linking SD with increased calcium demands, our western blot-confirmed transcriptomics studies in which SD increases the expression of VDAC1, a key MAM transcript essential for calcium transfer, together with documented studies linking ER

stress to calcium perturbations lead us to assume that calcium is essential to induce a cascade of events involving morphological changes. These mechanisms induce an increased mitochondrial production of oxidative radicals, which can damage proteins, lipids and other macromolecules including DNA; sudden increases in temperature inside the cell can lead to protein development, entanglement, and non-specific aggregation ("thermal shock") exacerbating ER stress. Depletion of mitochondrial calcium induces an increase in MAMs in order to promote calcium transfer from the ER to the mitochondria thus improving mitochondrial respiration in order to restore neuronal homeostasis and avoid further damage (Rizzuto et al. 2009). Morphology and interaction with other structures are modulated by the extent of proteostasis and calcium loss within the ER. Under these conditions of high stress mitochondria tend to form clusters, some groups found that cells containing cluster mitochondria lost cytochrome c from mitochondria and underwent caspase-mediated apoptosis (Huang et al. 2007). Furthermore, it has been shown that calcium deficiency within ER cisterns induces the formation of cortical ER, which migrates to the plasma membrane by inducing the formation of PAM, allowing calcium shuttling from the extracellular space to the mitochondria via ER (Buchanan et al. 2006). However, our studies revealed no significant changes in either the number or size of PAMs, and the findings on SD-induced neuronal apoptosis are controversial. In fact, it seems that neurons have in place a complex system of molecules and structures to manage cellular stress with the activation of a cascade of events to prevent further damage by preventing the progression of ER stress to its terminal deleterious phases. These complex mechanisms also include the phenomenon of "local sleep". Neurons, after a period of intense activation, present a behavioural state which closely resembles that of sleep, with patterns generally resemble NREM slow-wave sleep; this occurs while the animal is still fully conscious and functioning, although the associated abilities to the specific region of the brain in local sleep tend to decrease substantially. This phenomenon occurs also in Human (Tononi

et al. 2017, Nguyen et al. 2019). We have shown that ER stress induced by acute SD induces important metabolic and structural changes in the brain. However, it seems that the brain has devised evolutionary expedients to protect neurons from major damage at the expense of attention problems, deficits in performance and cognition. Furthermore, our studies have shown that increased MAMs were not only a consequence of SD, but they played some active role in regulating sleep itself, promoting shorter and less consolidated sleep.

9.2 Sleep deprivation and Myelin Fluidity

As mentioned in the previous paragraphs, SD heightens metabolism and protein synthesis leading to cellular stress and structural modifications. It has been demonstrated that these changes also involve myelin. Indeed, using electron and confocal microscopy Bellesi et al. recently showed that prolonged sleep restriction (~ 5 days) reduced myelin thickness and increased node of Ranvier length without affecting internodal length, thus suggesting that sleep loss can lead to plastic remodelling of myelin (Haswell et al. 2018). Poor sleep quality or short sleep duration are associated with changes in myelin structure also in humans; specifically, it has been shown that SD is associated with lower myelin content in the human neocortex (Toschi et al. 2021). These findings, together with studies that consistently report the upregulation of myelin-related genes during sleep, suggest that sleep is a window of opportunity during which myelination occurs (Gutierrez et al. 2004). How SD induces these changes is a hotspot for the field of sleep research as myelin is one of the most stable membranes in the body and SD is able to alter its maintenance, stability, and plasticity. In particular, myelin plasticity is gaining increasing recognition as an essential partner of synaptic plasticity, which mediates experience-dependent brain structure and function (Bellesi et al. 2019).

It is possible that prolonged wakefulness limits the deposition of new myelin due to the induction of ER stress. Indeed, there is evidence that a large number of oligodendrocyte-related genes (e.g. Derl3, Hsp5, Hsph1), which are upregulated by SD, are involved in the degradation of misfolded proteins and, more generally, participate in the unfolding process of protein response (Oda et al. 2006; Naidoo et al. 2007; Meares et al. 2008; Wang et al. 2009).

Furthermore, SD dramatically reduces the proliferation of myelin-producing oligodendrocytes in the CNS. Evidence in both rodents and humans seems to confirm that sleep loss is harmful to myelin, thus supporting the hypothesis that one function of sleep may actually be to keep white matter healthy. Our analysis of the oligodendroglia transcriptome revealed the upregulation of Fad3 in SD. Fad3 codes for a fatty acid desaturase which regulates the unsaturation of fatty acids and influences the fluidity of the membrane. We hypothesized that acute SD modifies the fluidity of the myelin membrane predisposing it to plastic changes since fluidity is an essential requirement for membrane plasticity. This finding is in line with our study of steady-state fluorescence spectroscopy in which we assessed a significant increase of fluidity in myelin membrane core in enriched samples of myelin of SD relative to S. Myelin membrane fluidity may exert a profound influence on cell functions by affecting the configuration, exposure, and diffusion of membrane components. Fluidity is a complex physicochemical feature that depends upon the mobility and order of membrane constituents (Singer et al. 1975). Changes in composition and molecular organization are the principal determinants of alterations of membrane fluidity observed in some pathological conditions(Singer et al. 1975) (Fiorini et al. 1990). For example, myelin lipid analysis revealed that diabetes alters the phospholipid, fatty acid and cholesterol content of myelin in a pattern that can modify membrane fluidity (Abbiati et al. 2012).

It is logical to assume that even SD acts by changing the expression and composition of some myelin lipids altering so the fluidity. A study demonstrated that in REM sleep-deprived animals there was an increase of DPH fluorescence polarization both in the microsome as well as in the synaptosome, except in the cerebellum, indicating that there was a generalized decrease in membrane fluidity. The alterations in membrane fluidity returned to baseline upon recovery from REM SD. This increase in membrane rigidity could be at least one of the possibilities for REM sleep loss-induced alterations in physiological phenomena including membrane-bound enzyme activities and receptor densities (Thakkar et al. 1995). The results of this study confirm that the SD is able to insinuate itself by altering the structure of the myelin; this instability (myelin too fluid or too rigid) can affect the functioning of the myelin itself. This finding might seem contrasting with our study in which after 6h of SD we detected an increase in fluidity in the myelin core while no significant difference at the membrane interface. In reality, in the study described above, the animals were continuously sleep deprived for a time ranging from 48 h to 96 h. This different time range allows us to speculate that in the initial stages of SD the body reacts by making the myelin membrane more fluid to counteract the myelin stiffening that SD induces. In fact, longer periods of SD instead induce a reduction in the fluidity of the membranes. Further studies need to be carried out to better verify the impact that SD has on the functioning and structure of myelin, given the fundamental role it plays within the CNS. Furthermore, just as myelination can be modified by local signalling at the axon-myelin interface, potentially adapting sheaths to support the metabolic needs and physiology of individual neurons so myelinated alterations can also involve synaptic plasticity, neuronal and glia cell activation (Hughes et al. 2021). It is important to explore these mechanisms especially in adolescents in which neurodevelopment is still in progress as damage to myelin is at the basis of numerous neurodegenerative diseases.

9.3 Characterization of Subcellular Organelles in Perisynaptic Astrocytic Processes

We described and quantified the distribution of organelles within PAPs in layers II of SS and AC cortices via EM volume. Our analysis revealed that in layer II > 75% of the ace spinous synapses are contacted by PAPs in the post-synaptic site. The synaptic coverage of these contacts reached the synaptic cleft in approximately 50% of all synapses in both the SS and AC cortices and these results are consistent with previous studies in different cortices and stages of development (Quairiaux et al. 2006; Bernardinelli et al. 2014; Bellesi et al. 2015; Gonzalez-Soriano et al. 2020). Interestingly, these results indicate that the concept of tripartite synapses is not always valid, in fact PAPs do not contact 50% of cortical synapses and of the synaptic cleft and 15% of all synapses are never contacted by PAP. astrocytic is carried out considering the diameter and is divided into branches, branchlets, and leaflets (Khakh and Sofroniew 2015). Our analysis revealed that 60% of the astrocytic processes that contact the synapses are leaflets, 37% are branchlets and only 3% are branches. The organelles observed within the empty PAPs are: full endosomes, full endosomes, phagosomes, mitochondria and ER cisterns. The organ number was found to increase with increasing diameter of the astrocytic processes, with leaflets looking less organelles per unit volume than larger processes. Furthermore, most of the leaves (~ 92%) were empty, while 1/3 of the twigs and about half of the branches had at least one organelle. It produced results consistent with our work which finds results that most subcellular organs are found in large processes (250> nm in our diameter) (Patrushev et al. 2013). We also observed that the five organelles identified within PAPs tend to form clusters. In particular, endosomes often appeared in association with phagosomes, while mitochondria were associated with ER cisterns. Our work disproves previous studies of glial ultrastructure in which PAPs are described as organless processes such as mitochondria, ERs or vesicular structures, although single vesicles, endosomes or mitochondria are occasionally mentioned (Derouiche et al. 2010) (Muller et al. 2014, Rusakov

et al. 2015). Indeed, we have shown that approximately 40% of cortical PAPs, which represent the vast majority of PAPs that contact synapses, contain one or more subcellular organelles. However, the idea that PAPs are not devoid of organelles has also been exposed by other groups. For example, more PAP organelles have recently been identified by applying new tissue fixation techniques, such as high pressure freezing and freezing replacement that better preserve the fine subcellular structure (Nikonenko et al. 2005, Ishida et al. 2006) (Cooper et al. 2010, Sahlender, Savtchouk et al. 2014) Similarly, vesicles within fine astrocytic processes have been described in several EM studies conducted on "gliosomes", an in vitro preparation of glial subcellular particles often used to study the uptake and release mechanisms of the astrocytic transmitter (Bonifacino et al. 2009; Frattaroli et al. 2015).

Through the use of array tomography and serial block face scanning electron microscope (SBF-SEM) they revealed further morphological characteristics of the astrocytic processes and highlighted some new and relevant astrocytic properties (Emery et al. 2008; Clarke et al. 2013, Kim et al. 2014, Bellesi et al. 2015, de Vivo et al. 2017). Specifically, it has been discovered that PAPs are capable of structurally remodelling synapses by phagocytic synaptic elements or portions of them (Chung et al. 2013; Bellesi et al. 2017, Kim et al. 2021). This phagocytic activity requires dedicated intracellular machinery that engulfs, transports, and degrades material within the PAPs. It is not surprising therefore that more than 60% of the organelles that we described within PAPs are related to phagocytosis (EE, FE, and PH). These organelles tend to be associated, thus suggesting that they may be functionally linked and participate in the same biological process (i.e., phagocytosis). Similarly, mitochondria and ER cisternae, which account for about 40% of all the organelles, were often associated within the PAPs. Recent studies have indicated that the interaction between ER cisternae and mitochondria may promote specific astrocytic functions such as brain tissue repair (Engelhardt et al. 2020). ER cisternae represent the intracellular source of calcium, and calcium activity in astrocytes is

largely compartmented and preponderantly occurs in PAPs, while the soma is mostly inactive (Savtchouk et al. 2017). Calcium is released intracellularly upon astrocyte activation and concomitant synaptic firing and it is involved in numerous biological processes, including astrocyte metabolic responses and PAPs structural plasticity (O'Donnell et al. 2013, Verkhratsky et al. 2018). Therefore, the presence of ER cisternae in PAPs guarantees calcium availability to allow these processes to occur locally. However, since we found evidence of ER cisternae in only ~45% of the PAPs, other mechanisms (e.g., calcium exchangers) must be in place to allow calcium dynamics in ER-free PAPs (Héja and Kardos, 2020). It is well recognized that PAPs are not only structurally associated with synapses, they fulfil homeostatic, metabolic, and regulatory functions (Kimelberg et al. 2007, Bouzier-Sore et al. 2007, Perea et al. 2010) . Therefore, the functional state of the synapses could influence the functions of the PAPs and vice versa. Although it is difficult to identify certain morphological characteristics that are associated with precise synaptic functional states, there are some synaptic morphological characteristics that define specific categories of synapses that can behave differently in terms of activation activity or plasticity. This is the case, for example, of synapses containing a spinal apparatus or a presynaptic mitochondrion. The spine apparatus plays a role in synaptic plasticity as synaptopodine-deficient mice lacking these organelles have been observed to exhibit deficits in long-term potentiation and spatial learning. (Jedlicka et al. 2008). Similarly, presynaptic mitochondria are found in axon terminals that are stable and less prone to change in size (Johnson et al. 2019). Therefore, it is plausible to hypothesize that synapses characterized by the presence of a spinal apparatus or a presynaptic mitochondrion could possess different plastic capacities from those which these organelles do not have. We therefore decided to analyze the distribution of organelles in the PAP of the ace-spinous synapses with or without spinal apparatus and presynaptic mitochondria. The distribution was found to be broadly similar between these types of synapses, with the exception of phagosomes

and ER cisterns. It is possible that the distribution of PAPs may be affected by synapses close to but not necessarily in contact with them. In other words, the distribution of organelles within PAPs may depend on the general local environment and not be strictly dependent on opposing synapses. Furthermore, the presence of presynaptic or spinal mitochondria can induce changes so small that they cannot be detected in the surrounding PAPs with our method. Third, the distribution of organelles is sensitive to synaptic characteristics that we have not considered or are not associated with a specific morphological phenotype (for example, the amount of neurotransmitter released or the extent of ionic changes). We found differences in the various types of synapses relative to the density of phagosomes and ER cisterns. Phagosomes were more numerous in synapses without the spinal apparatus, while ER cisterns were more represented in synapses without presynaptic mitochondria. We can hypothesize that both phagosomes and ER in astrocytes could be useful for plastic remodeling of young synapses that still show low levels of pre- and postsynaptic stability. Increasing evidence in recent years is showing that astrocytes exhibit significant variability in gene expression and physiology within and between brain regions (Miller et al. 2018). The surprising heterogeneity of astrocytes has been described between different layers within the same region and different regions of the brain (hippocampus vs. cerebral cortex)   (Hirase et al. 2008, Taniguchi et al. 2009, Yu et al. 2017, Liddelow et al. 2018). In our study, we sampled PAP from layer II of the SS and AC cortices, two regions involved in different functions and belonging to a different hierarchical category. We did not observe any difference in the distribution of PAP organelles between these cortical regions. Thus, we can hypothesize that the composition of organelles in PAPs is not a heterogeneous feature, at least across the surface layers of the neocortex. In conclusion, this study found that an important number of organelles in cortical PAPs are related to phagocytosis, a cellular function that is it has only recently been described in astrocytes. It is logical to think that the distribution of the organelles in the PAPs does not depend on some

specific morphological characteristics of the synapses that the PAPs are enveloping, therefore it remains to understand what determines their density and spatial organization. However, our study has some limited ones. First, SBF-SEM requires specific EM staining enriched in heavy metals, which contrasts with lipids facilitating the detection of membranous organelles but can also limit the visualization of protein-enriched structures. These limitations may have caused reduced detection of synaptic micro-vesicles of 30-40 nm that were previously identified in PAPs using other methods (Bergersen et al. 2007, Morland et al. 2012, Frattaroli et al. 2015). These vesicles are much smaller than our EEs (80-150 nm), which probably belong to a completely different category of intracellular PAP organelles with a function that remains to be elucidated. Furthermore, we have focused our attention only on PAPs in contact with the Axis-spinous synapses of layer II, so the information gathered for the neocortex is incomplete and requires further investigation that extends to other cortical layers and types of synapses.
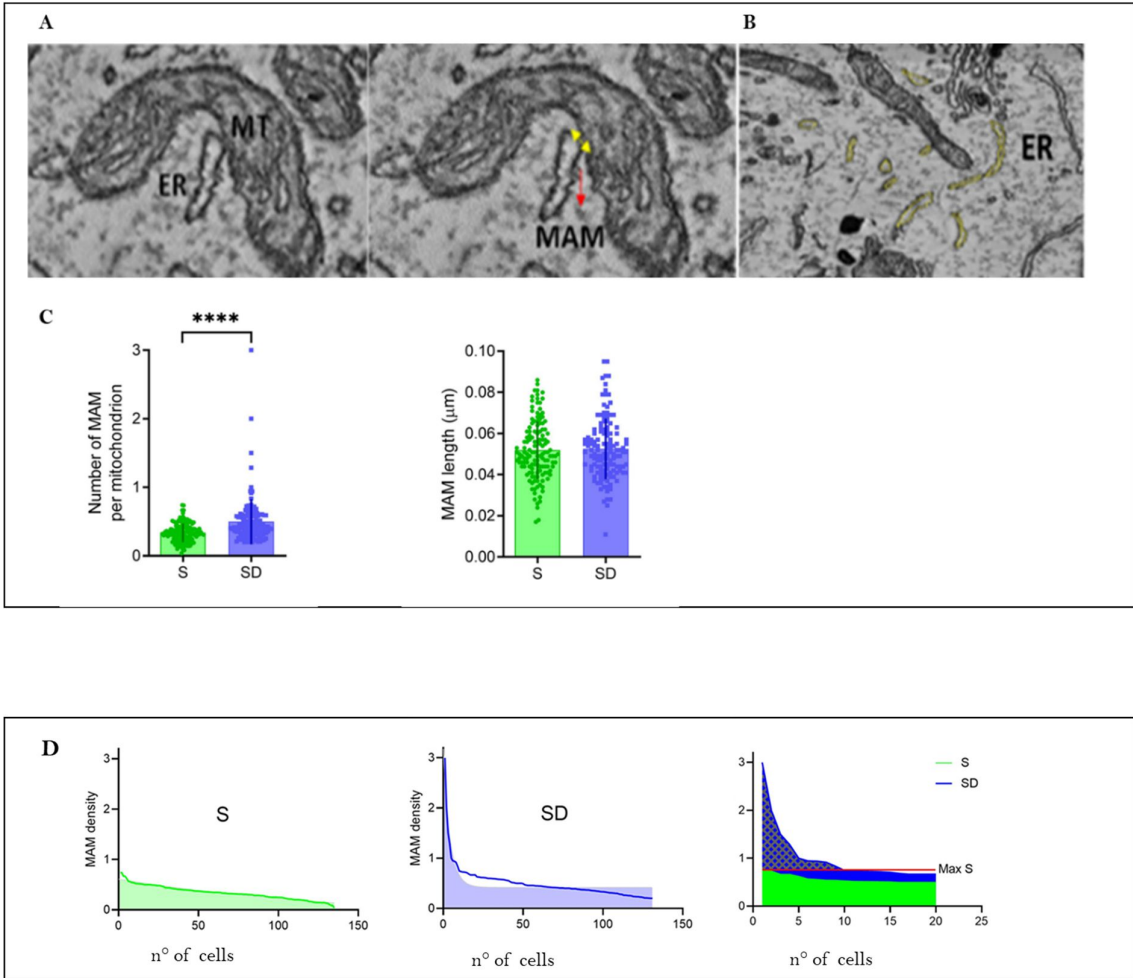
Figure 1: (**A**) MT: mitochondrion , ER: endoplasmic reticulum, MAM: Membranes associated with mitochondria, (**B**) Manual segmentation and analysis of ER, Scale bar:500nm, (**C**) Length of MAMs and Number of MAMs, quantified as number per mitochondrion, in S and SD, (**D**) MAMs density per Cells number
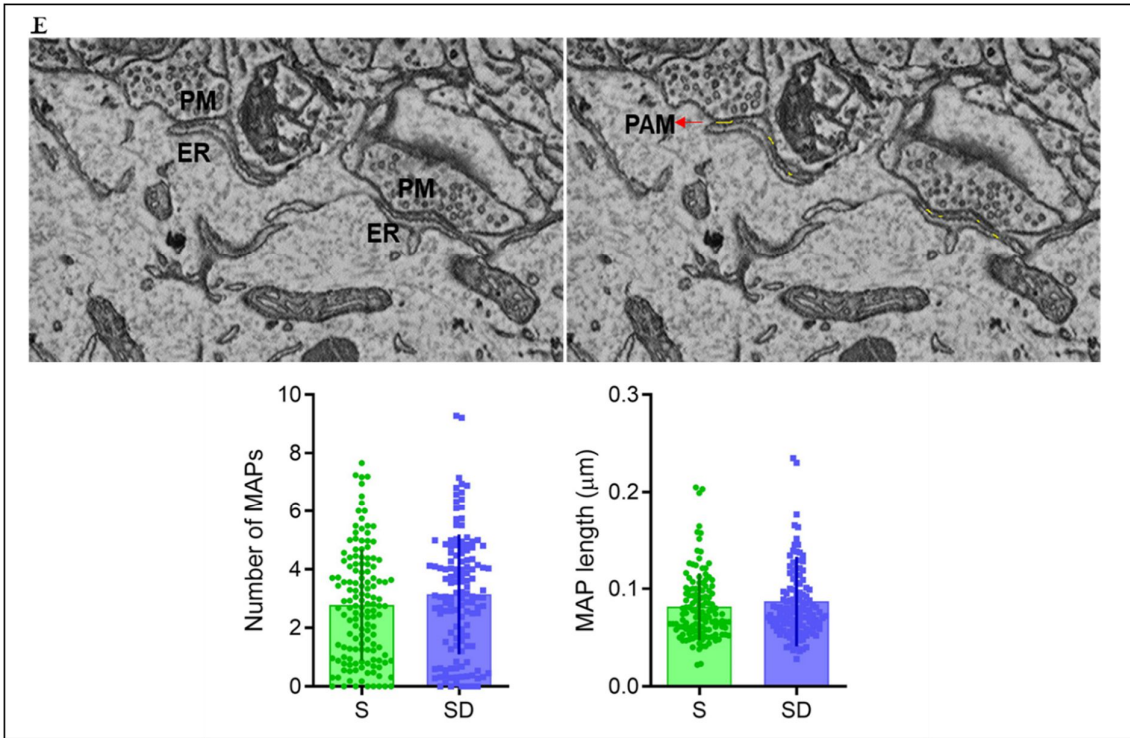
Figure 1: (E) Above PM: Plasma membrane, ER: Endoplasmic Reticulum, PAM: Plasma membrane associated membranes, Scale Bar: 500 nm. Below: Graph Length and Number of PAMs in S and SD.
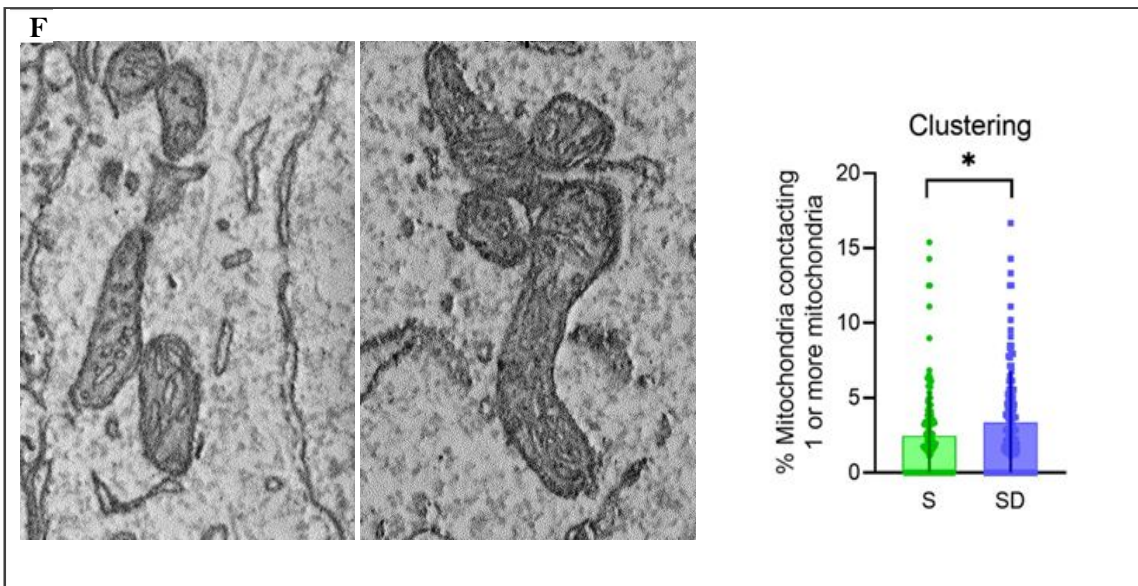

Figure 1: (F) On the right, images of mitochondrial clusters, on the left, the number of mitochondrial clusters in relation to S and SD
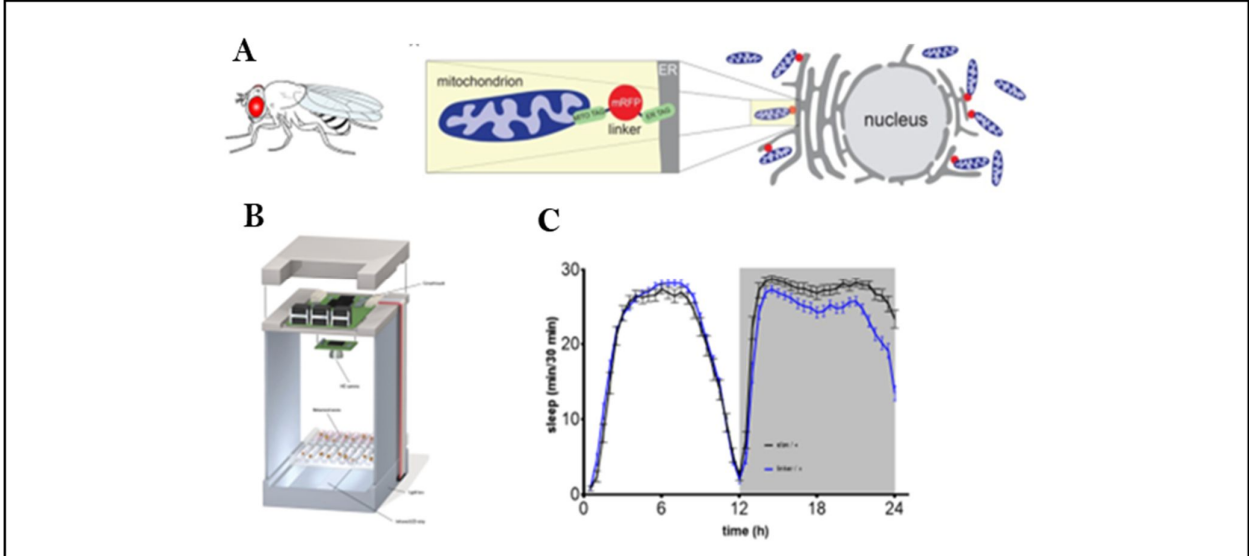
Figure 2 (A-C): Male mutant flies (overexpression of MAMs linker) and both parent control housed in a chamber in monitor chamber for 3-4 days in order to have a reliable measure of their sleep and wake.
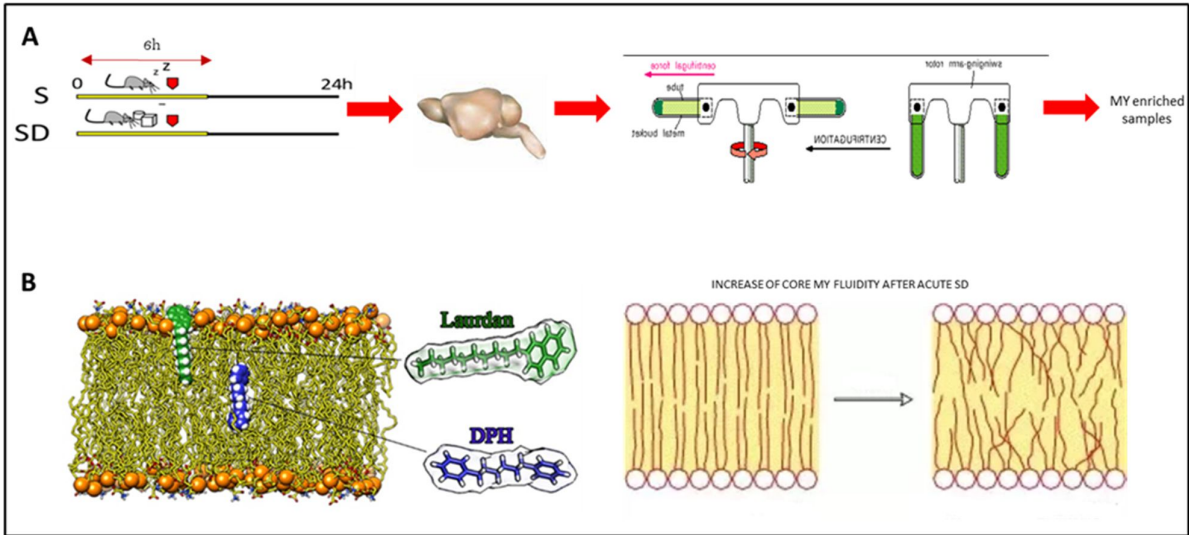

Figure 3: (A) A brief descriptive scheme of how myelin-enriched samples were obtained. Brains of SD mice were collected after dislocation and they were subjected to several steps described by Larocca in his paper. **(B)** Two florescent probes were used: Laurdan located at hydrophobic-hydrophilic interface of the membrane and DPH located at hydrophobic-hydrophilic interface of the membrane. Our result revealed a significant increase in myelin membrane core in SD relative to S.
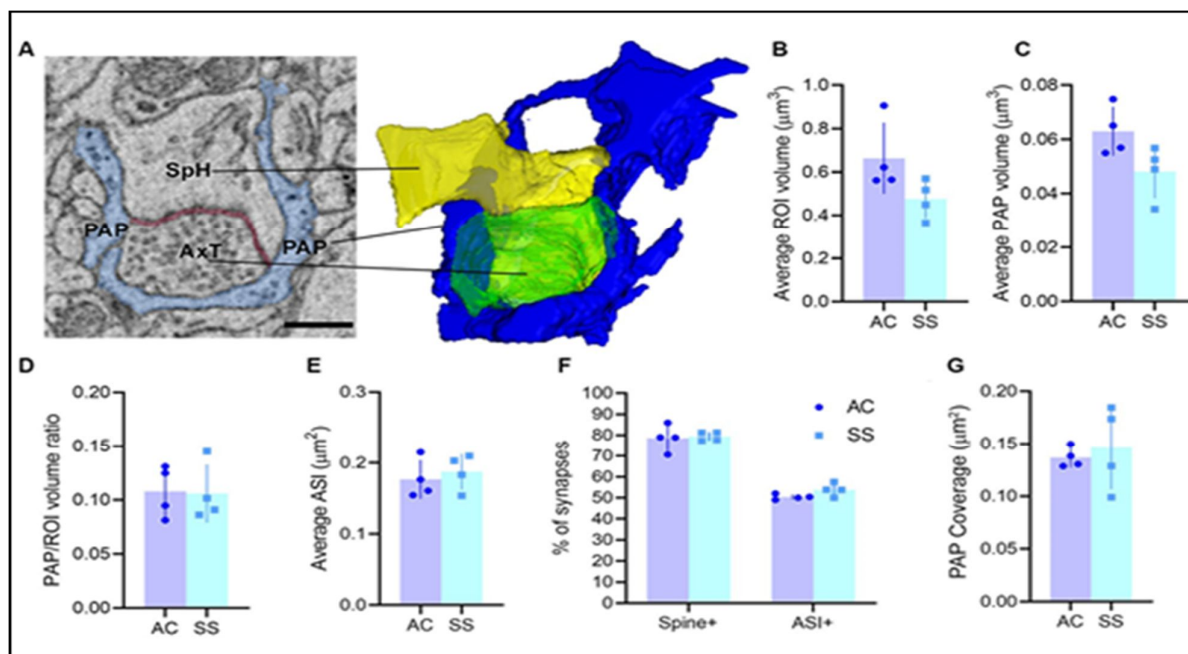
FIGURE 4 | (A) Example of region of interest (ROI) showing an axo-spinous synapse with perisynaptic astrocytic process (PAP;blue), axon terminal (AxT), spine head (SpH), axon-spine interface (ASI, red), and relative 3D reconstruction. Scale bar: 400 nm. **(B,C)** Average ROI and PAP volumes, respectively. (D) Ratio betweenPAP and ROI volumes. **(E)** Average ASI size. **(F)** Percentage of synapses contacting the spine (spine+) and the synaptic cleft (ASI+). **(G)** Synaptic coverage as measured by the size of the interfacing surface between the PAP and the spine head. In panels **(B–G)** AC and SS refer to anterior cingulate and somatosensory cortex (paired t-test, n = 4).
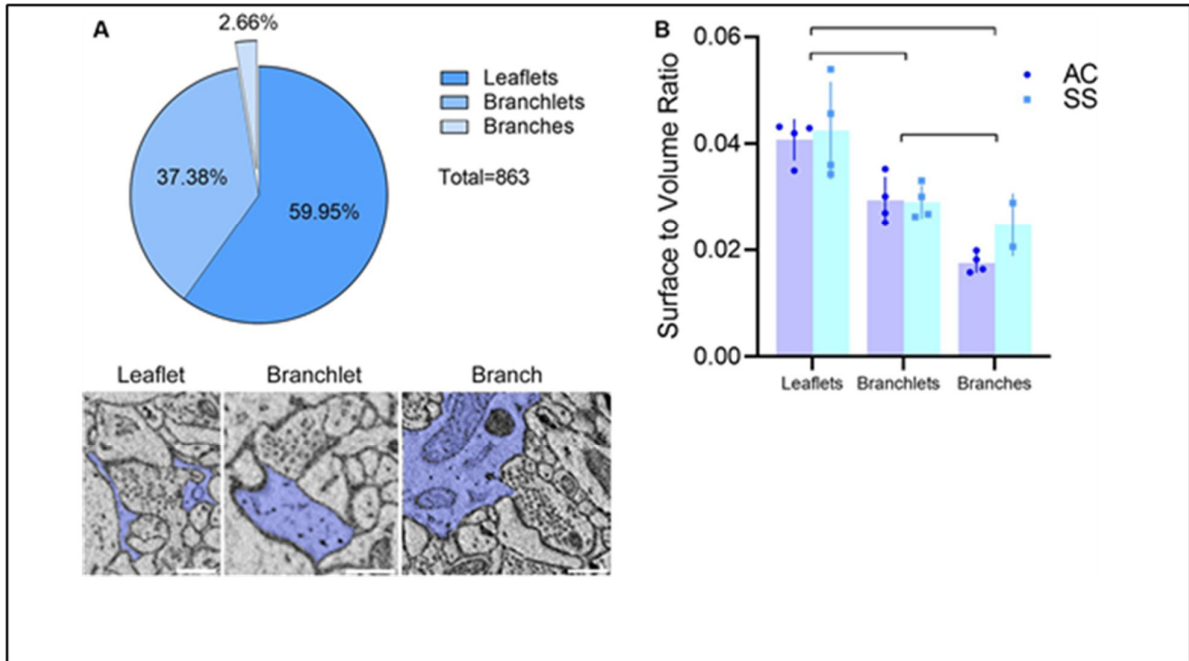
FIGURE 5 | (A) Top: PAP composition in our dataset (*n* = 863, four animals). Bottom: examples of the leaflet, branchlet, and branch depicted in blue and surrounding an axo-spinous synapse. The scale bar is 350 nm for all panels. **(B)** Average surface-to-volume ratio values in AC and SS (mixed-effects analysis, *n* = 4). Lines indicate significant pairwise comparisons (*p* < 0.05, Bonferroni corrected).
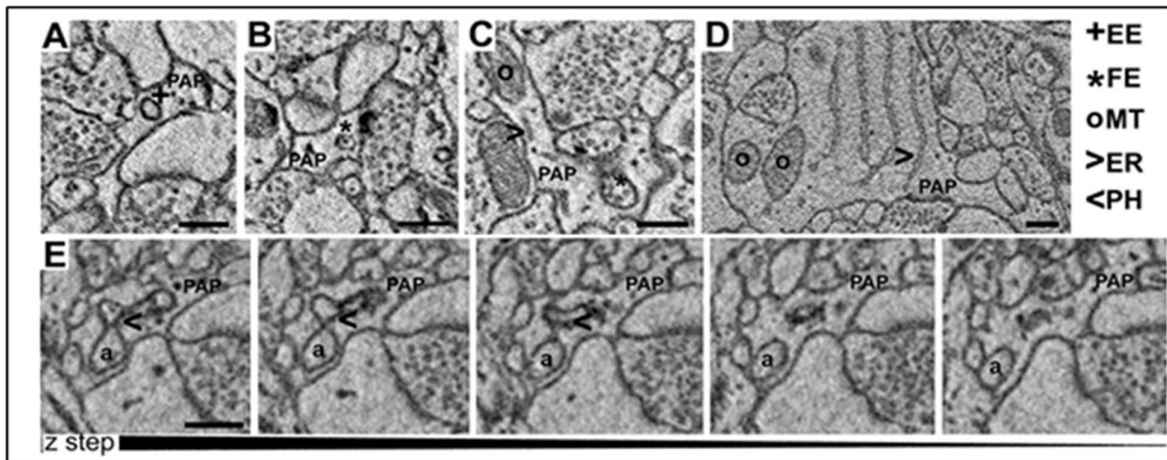

FIGURE 6 | (A–D) Examples of empty endosomes (EE), full endosomes (FE), mitochondria (MT), ER-cisternae (ER). **(E)** Axon (a) being engulfed by a PAP caught in several consecutive *z*-steps showing the formation of the phagosome (PH). Scale bar is 300 nm for all panels.
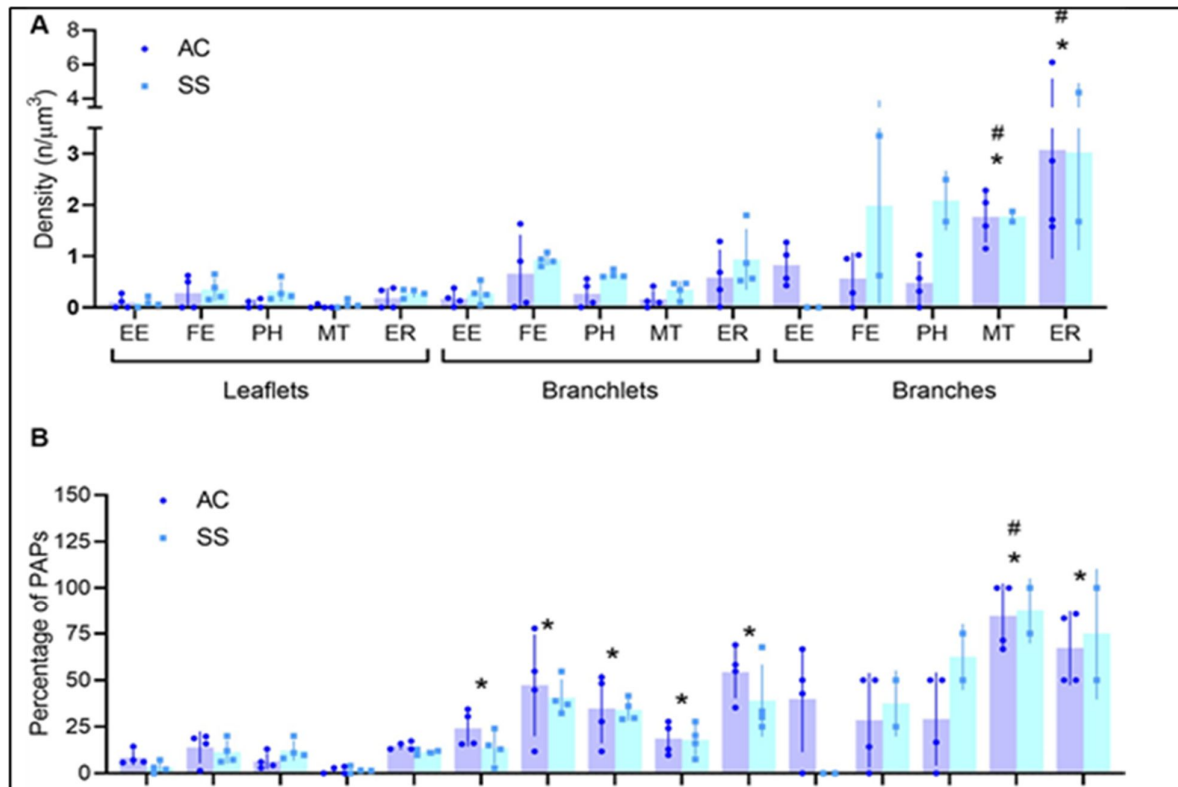
FIGURE 7 | (A,B) Quantification of PAP subcellular organelle distribution (A) and percentage of perisynaptic astrocytic processes (PAPS) displaying at least one organelle (**B**). All data are segregated for leaflets, branchlets, and branches ($n = 4$). Empty endosomes (EE), full endosomes (FE), phagosome (PH), mitochondria (MT), and ER cisternae (ER) for all panels. *Indicates significant pairwise comparisons (mixed-effects analysis, $p < 0.05$, Bonferroni corrected) relative to leaflets, whereas, the #indicates significant pairwise comparisons (mixed-effects analysis, $p < 0.05$, Bonferroni corrected) relative to branchlets.
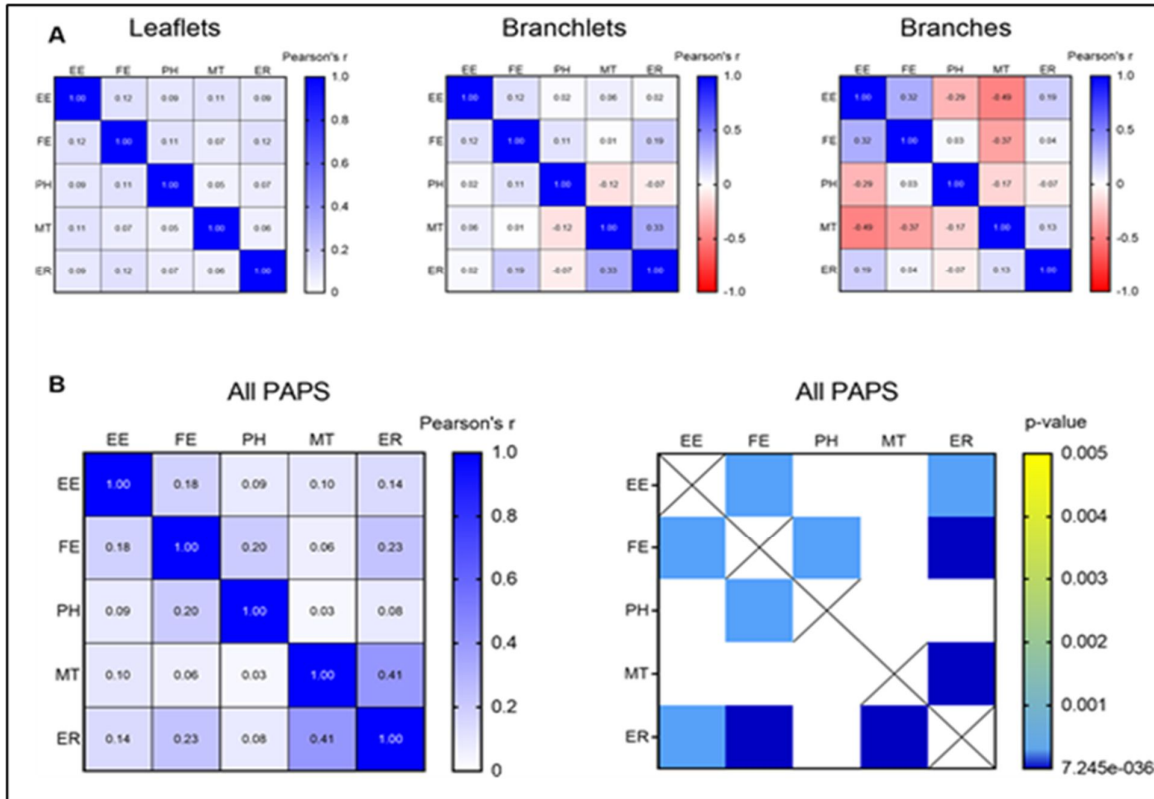
FIGURE 8 | (A) Correlation matrix indicating the strength of the correlation between all the described organelles in leaflets, branchlets, and branches separately. **(B)** Correlation matrix indicating strength (left) and significance (right) of the correlation between all the described organelles in all the PAPs pooled together. Only significant correlations after Bonferroni's correction for multiple comparisons are displayed. Empty endosomes (EE), full endosomes (FE), phagosome (PH), mitochondria (MT), and ER cisternae (ER) for all panels.
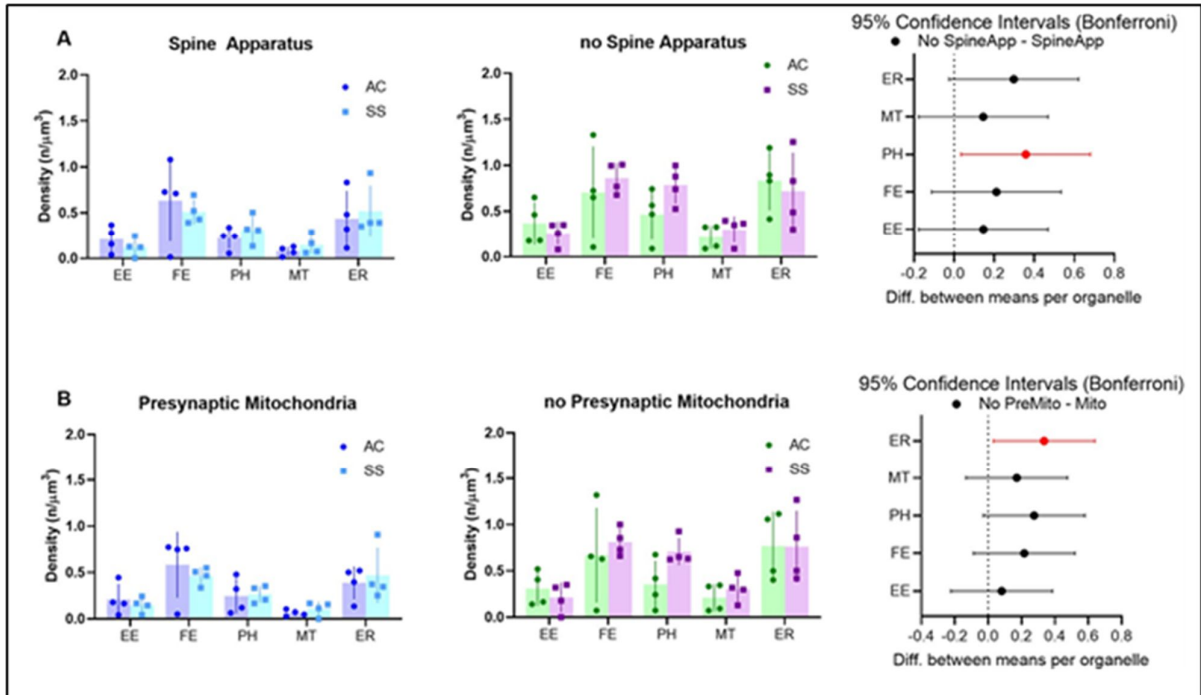
FIGURE 9| **(A)** Subcellular organelle distribution in PAPs surrounding synapses with (left) or without (middle) spine apparatus and relative statistical analysis (right, rmANOVA followed by *post hoc* Bonferroni tests, *n* = 4). **(B)** Subcellular organelle distribution in PAPs surrounding synapses with (left) or without (middle) presynaptic mitochondrion and relative statistical analysis (right, rmANOVA followed by *post hoc* Bonferroni tests *n* = 4). Empty endosomes (EE), full endosomes (FE), phagosome (PH), mitochondria (MT), and ER cisternae (ER) for all panels.

References:

Akagi, T., et al. (2006). "Improved methods for ultracryotomy of CNS tissue for ultrastructural and immunogold analyses." J Neurosci Methods **153**(2): 276-282.

Anunciado-Koza, R. P., et al. (2011). "Inactivation of the mitochondrial carrier SLC25A25 (ATP-Mg2+/Pi transporter) reduces physical endurance and metabolic efficiency in mice." J Biol Chem **286**(13): 11659-11671.

Aserinsky, E. and N. Kleitman (1953). "Regularly occurring periods of eye motility, and concomitant phenomena, during sleep." Science **118**(3062): 273-274.

Bagatolli, L. A. and E. Gratton (1999). "Two-photon fluorescence microscopy observation of shape changes at the phase transition in phospholipid giant unilamellar vesicles." Biophys J **77**(4): 2090-2101.

Bellesi, M., et al. (2017). "Sleep Loss Promotes Astrocytic Phagocytosis and Microglial Activation in Mouse Cerebral Cortex." J Neurosci **37**(21): 5263-5273.

Bellesi, M., et al. (2015). "Effects of sleep and wake on astrocytes: clues from molecular and ultrastructural studies." BMC Biol **13**: 66.

Bellesi, M., et al. (2018). "Myelin modifications after chronic sleep loss in adolescent mice." Sleep **41**(5).

Bellesi, M., et al. (2013). "Effects of sleep and wake on oligodendrocytes and their precursors." J Neurosci **33**(36): 14288-14300.

Bergersen, L. H., et al. (2012). "Immunogold detection of L-glutamate and D-serine in small synaptic-like microvesicles in adult hippocampal astrocytes." Cereb Cortex **22**(7): 1690-1697.

Bernardinelli, Y., et al. (2014). "Astrocyte-synapse structural plasticity." Neural Plast **2014**: 232105.

Besedovsky, L., et al. (2019). "The Sleep-Immune Crosstalk in Health and Disease." Physiol Rev **99**(3): 1325-1380.

Bindocci, E., et al. (2017). "Three-dimensional Ca(2+) imaging advances understanding of astrocyte biology." Science **356**(6339).

Boneh, A. (2006). "Regulation of mitochondrial oxidative phosphorylation by second messenger-mediated signal transduction mechanisms." Cell Mol Life Sci **63**(11): 1236-1248.

Bravo, R., et al. (2012). "Endoplasmic reticulum: ER stress regulates mitochondrial bioenergetics." Int J Biochem Cell Biol **44**(1): 16-20.

Bravo, R., et al. (2011). "Increased ER-mitochondrial coupling promotes mitochondrial respiration and bioenergetics during early phases of ER stress." J Cell Sci **124**(Pt 13): 2143-2152.

Brown, M. K., et al. (2014). "Aging induced endoplasmic reticulum stress alters sleep and sleep homeostasis." Neurobiol Aging **35**(6): 1431-1441.

Cahoy, J. D., et al. (2008). "A transcriptome database for astrocytes, neurons, and oligodendrocytes: a new resource for understanding brain development and function." J Neurosci **28**(1): 264-278.

Cermenati, G., et al. (2012). "Diabetes-induced myelin abnormalities are associated with an altered lipid pattern: protective effects of LXR activation." J Lipid Res **53**(2): 300-310.

Cervetto, C., et al. (2015). "Calcium-permeable AMPA receptors trigger vesicular glutamate release from Bergmann gliosomes." Neuropharmacology **99**: 396-407.

Chandra, D., et al. (2007). "Cytosolic accumulation of HSP60 during apoptosis with or without apparent mitochondrial release: evidence that its pro-apoptotic or pro-survival functions involve differential interactions with caspase-3." J Biol Chem **282**(43): 31289-31301.

Chung, W. S., et al. (2013). "Astrocytes mediate synapse elimination through MEGF10 and MERTK pathways." Nature **504**(7480): 394-400.

Cirelli, C. (2006). "Cellular consequences of sleep deprivation in the brain." Sleep Med Rev **10**(5): 307-321.

Cirelli, C., et al. (2006). "Changes in brain gene expression after long-term sleep deprivation." J Neurochem **98**(5): 1632-1645.

Cirelli, C., et al. (1999). "No evidence of brain cell degeneration after long-term sleep deprivation in rats." Brain Res **840**(1-2): 184-193.

Cirelli, C. and G. Tononi (1998). "Changes in anti-phosphoserine and anti-phosphothreonine antibody binding during the sleep-waking cycle and after lesions of the locus coeruleus." Sleep Res Online **1**(1): 11-18.

Clarke, L. E., et al. (2018). "Normal aging induces A1-like astrocyte reactivity." Proc Natl Acad Sci U S A **115**(8): E1896-e1905.

D'Eletto, M., et al. (2018). "Transglutaminase Type 2 Regulates ER-Mitochondria Contact Sites by Interacting with GRP75." Cell Rep **25**(13): 3573-3581.e3574.

Davis, C. H., et al. (2014). "Transcellular degradation of axonal mitochondria." Proc Natl Acad Sci U S A **111**(26): 9633-9638.

De Havas, J. A., et al. (2012). "Sleep deprivation reduces default mode network connectivity and anti-correlation during rest and task performance." Neuroimage **59**(2): 1745-1751.

de Vivo, L. and M. Bellesi (2019). "The role of sleep and wakefulness in myelin plasticity." Glia **67**(11): 2142-2152.

Ding, F., et al. (2013). "α1-Adrenergic receptors mediate coordinated Ca2+ signaling of cortical astrocytes in awake, behaving mice." Cell Calcium **54**(6): 387-394.

Durmer, J. S. and D. F. Dinges (2005). "Neurocognitive consequences of sleep deprivation." Semin Neurol **25**(1): 117-129.

Elvsåshagen, T., et al. (2015). "Widespread changes in white matter microstructure after a day of waking and sleep deprivation." PloS one **10**(5): e0127351.

Endres, K. and S. Reinhardt (2013). "ER-stress in Alzheimer's disease: turning the scale?" Am J Neurodegener Dis **2**(4): 247-265.

Fiorini, R., et al. (1990). "Steady state fluorescence polarization and Fourier transform infrared spectroscopy studies on membranes of functionally senescent human erythrocytes." Biochem Int **20**(4): 715-724.

Furuya, K., et al. (2006). "Intracerebroventricular delivery of dominant negative prion protein in a mouse model of iatrogenic Creutzfeldt-Jakob disease after dura graft transplantation." Neurosci Lett **402**(3): 222-226.

Genoud, C., et al. (2006). "Plasticity of astrocytic coverage and glutamate transporter expression in adult mouse cortex." PLoS Biol **4**(11): e343.

Giorgi, C., et al. (2009). "Structural and functional link between the mitochondrial network and the endoplasmic reticulum." Int J Biochem Cell Biol **41**(10): 1817-1827.

Göbel, J., et al. (2020). "Mitochondria-Endoplasmic Reticulum Contacts in Reactive Astrocytes Promote Vascular Remodeling." Cell Metab **31**(4): 791-808.e798.

Héja, L. and J. Kardos (2020). "NCX activity generates spontaneous Ca(2+) oscillations in the astrocytic leaflet microdomain." Cell Calcium **86**: 102137.

Heller, J. P. and D. A. Rusakov (2015). "Morphological plasticity of astroglia: Understanding synaptic microenvironment." Glia **63**(12): 2133-2151.

Heverin, M., et al. (2012). "Proteomic analysis of 14-3-3 zeta binding proteins in the mouse hippocampus." Int J Physiol Pathophysiol Pharmacol **4**(2): 74-83.

Hibar, D. P., et al. (2018). "Cortical abnormalities in bipolar disorder: an MRI analysis of 6503 individuals from the ENIGMA Bipolar Disorder Working Group." Mol Psychiatry **23**(4): 932-942.

Hinard, V., et al. (2012). "Key electrophysiological, molecular, and metabolic signatures of sleep and wakefulness revealed in primary cortical cultures." J Neurosci **32**(36): 12506-12517.

Hughes, A. N. (2021). "Glial Cells Promote Myelin Formation and Elimination." Front Cell Dev Biol **9**: 661486.

Institute of Medicine Committee on Sleep, M. and Research (2006). The National Academies Collection: Reports funded by National Institutes of Health. Sleep Disorders and Sleep Deprivation: An Unmet Public Health Problem. H. R. Colten and B. M. Altevogt. Washington (DC), National Academies Press (US)

Copyright © 2006, National Academy of Sciences.

Jiang, C., et al. (2014). "Diurnal microstructural variations in healthy adult brain revealed by diffusion tensor imaging." PloS one **9**(1): e84822.

John Lin, C. C., et al. (2017). "Identification of diverse astrocyte populations and their malignant analogs." Nat Neurosci **20**(3): 396-405.

Jourdain, P., et al. (2007). "Glutamate exocytosis from astrocytes controls synaptic strength." Nat Neurosci **10**(3): 331-339.

Kaneko, K. and N. S. Hachiya (2006). "The alternative role of 14-3-3 zeta as a sweeper of misfolded proteins in disease conditions." Med Hypotheses **67**(1): 169-171.

Kemp, P. J., et al. (2002). "Airway chemotransduction: from oxygen sensor to cellular effector." Am J Respir Crit Care Med **166**(12 Pt 2): S17-24.

Khakh, B. S. and M. V. Sofroniew (2015). "Diversity of astrocyte functions and phenotypes in neural circuits." Nat Neurosci **18**(7): 942-952.

Ki, S. H., et al. (2010). "Interleukin-22 treatment ameliorates alcoholic liver injury in a murine model of chronic-binge ethanol feeding: role of signal transducer and activator of transcription 3." Hepatology **52**(4): 1291-1300.

Kikuchi, T., et al. (2020). "Volume Electron Microscopy Study of the Relationship Between Synapses and Astrocytes in the Developing Rat Somatosensory Cortex." Cereb Cortex **30**(6): 3800-3819.

Killgore, W. D. (2010). "Effects of sleep deprivation on cognition." Prog Brain Res **185**: 105-129.

Kimelberg, H. K. (2007). "Supportive or information-processing functions of the mature protoplasmic astrocyte in the mammalian CNS? A critical appraisal." Neuron Glia Biol **3**(3): 181-189.

Kozieł, K., et al. (2009). "Plasma membrane associated membranes (PAM) from Jurkat cells contain STIM1 protein is PAM involved in the capacitative calcium entry?" Int J Biochem Cell Biol **41**(12): 2440-2449.

Krueger, J. M. (2008). "The role of cytokines in sleep regulation." Curr Pharm Des **14**(32): 3408-3416.

Krueger, J. M., et al. (2019). "Local sleep." <u>Sleep Med Rev</u> **43**: 14-21.

Krueger, J. M., et al. (2008). "Sleep as a fundamental property of neuronal assemblies." <u>Nat Rev Neurosci</u> **9**(12): 910-919.

Lee, J. H., et al. (2021). "Astrocytes phagocytose adult hippocampal synapses for circuit homeostasis." <u>Nature</u> **590**(7847): 612-617.

Lees, R. M., et al. (2019). "Presynaptic Boutons That Contain Mitochondria Are More Stable." <u>Front Synaptic Neurosci</u> **11**: 37.

Lentz, B. R. (1989). "Membrane "fluidity" as detected by diphenylhexatriene probes." <u>Chemistry and Physics of Lipids</u> **50**(3): 171-190.

Liu, M., et al. (2017). "Sirt6 deficiency exacerbates podocyte injury and proteinuria through targeting Notch signaling." <u>Nat Commun</u> **8**(1): 413.

Mackiewicz, M., et al. (2009). "What are microarrays teaching us about sleep?" <u>Trends Mol Med</u> **15**(2): 79-87.

Maret, S., et al. (2007). "Homer1a is a core brain molecular correlate of sleep loss." <u>Proc Natl Acad Sci U S A</u> **104**(50): 20090-20095.

Milanese, M., et al. (2009). "Glutamate release from astrocytic gliosomes under physiological and pathological conditions." <u>Int Rev Neurobiol</u> **85**: 295-318.

Miller, S. J. (2018). "Astrocyte Heterogeneity in the Adult Central Nervous System." <u>Front Cell Neurosci</u> **12**: 401.

Möbius, W., et al. (2010). "Electron microscopy of the mouse central nervous system." <u>Methods Cell Biol</u> **96**: 475-512.

Mongrain, V., et al. (2010). "Separating the contribution of glucocorticoids and wakefulness to the molecular and electrophysiological correlates of sleep homeostasis." <u>Sleep</u> **33**(9): 1147-1157.

Movshovich, R., et al. (2004). "Electron-spin domains: magnetic enhancement of superconductivity." <u>Nature</u> **427**(6977): 802; discussion 802.

Naidoo, N., et al. (2005). "Sleep deprivation induces the unfolded protein reponse in mouse cerebral cortex." Journal of neurochemistry **92**: 1150-1157.

Naidoo, N., et al. (2005). "Sleep deprivation induces the unfolded protein response in mouse cerebral cortex." J Neurochem **92**(5): 1150-1157.

Nath Mallick, B., et al. (1995). "Rapid eye movement sleep deprivation decreases membrane fluidity in the rat brain." Neuroscience Research **22**(1): 117-122.

Norton, W. T. (1974). "Isolation of myelin from nerve tissue." Methods Enzymol **31**: 435-444.

Oakes, S. A. and F. R. Papa (2015). "The role of endoplasmic reticulum stress in human pathology." Annu Rev Pathol **10**: 173-194.

Pace-Schott, E. F. and J. A. Hobson (2002). "The neurobiology of sleep: genetics, cellular physiology and subcortical networks." Nat Rev Neurosci **3**(8): 591-605.

Palagini, L., et al. (2013). "Sleep loss and hypertension: a systematic review." Curr Pharm Des **19**(13): 2409-2419.

Parasassi, T., et al. (1993). "Absence of lipid gel-phase domains in seven mammalian cell lines and in four primary cell types." Biochim Biophys Acta **1153**(2): 143-154.

Patergnani, S., et al. (2011). "Calcium signaling around Mitochondria Associated Membranes (MAMs)." Cell Commun Signal **9**: 19.

Patrushev, I., et al. (2013). "Subcellular location of astrocytic calcium stores favors extrasynaptic neuron-astrocyte communication." Cell Calcium **54**(5): 343-349.

Pellerin, L., et al. (2007). "Activity-dependent regulation of energy metabolism by astrocytes: an update." Glia **55**(12): 1251-1262.

Perea, G. and A. Araque (2010). "GLIA modulates synaptic transmission." Brain Res Rev **63**(1-2): 93-102.

Porter, N., et al. (2012). "Hippocampal CA1 Transcriptional Profile of Sleep Deprivation: Relation to Aging and Stress." PloS one **7**: e40128.

Pouliquin, P. and A. F. Dulhunty (2009). "Homer and the ryanodine receptor." Eur Biophys J **39**(1): 91-102.

Qian, Y., et al. (2016). "Inhibition of inflammation and oxidative stress by an imidazopyridine derivative X22 prevents heart injury from obesity." J Cell Mol Med **20**(8): 1427-1442.

Rechtschaffen, A. (1998). "Current perspectives on the function of sleep." Perspect Biol Med **41**(3): 359-390.

Rechtschaffen, A. and B. M. Bergmann (2002). "Sleep Deprivation in the Rat: An Update of the 1989 Paper." Sleep **25**(1): 18-24.

Reichenbach, A., et al. (2010). "Morphology and dynamics of perisynaptic glia." Brain Res Rev **63**(1-2): 11-25.

Sahlender, D. A., et al. (2014). "What do we know about gliotransmitter release from astrocytes?" Philos Trans R Soc Lond B Biol Sci **369**(1654): 20130592.

Sämann, P. G., et al. (2010). "Increased sleep pressure reduces resting state functional connectivity." Magma **23**(5-6): 375-389.

Sano, R. and J. C. Reed (2013). "ER stress-induced cell death mechanisms." Biochim Biophys Acta **1833**(12): 3460-3470.

Sassano, M. L., et al. (2017). "Mitochondria-Associated Membranes As Networking Platforms and Regulators of Cancer Cell Fate." Front Oncol **7**: 174.

Scharf, M. T., et al. (2008). "The energy hypothesis of sleep revisited." Prog Neurobiol **86**(3): 264-280.

Schon, E. A. (2018). "Bioenergetics through thick and thin." Science **362**(6419): 1114-1115.

Schröder, M. (2008). "Endoplasmic reticulum stress responses." Cell Mol Life Sci **65**(6): 862-894.

Schuck, S., et al. (2009). "Membrane expansion alleviates endoplasmic reticulum stress independently of the unfolded protein response." J Cell Biol **187**(4): 525-536.

Shannon, B. J., et al. (2013). "Morning-evening variation in human brain metabolism and memory circuits." J Neurophysiol **109**(5): 1444-1456.

Shigiyama, F., et al. (2018). "Mechanisms of sleep deprivation-induced hepatic steatosis and insulin resistance in mice." Am J Physiol Endocrinol Metab **315**(5): E848-e858.

Shoshan-Barmatz, V., et al. (2018). "VDAC1, mitochondrial dysfunction, and Alzheimer's disease." Pharmacol Res **131**: 87-101.

Siclari, F. and G. Tononi (2017). "Local aspects of sleep and wakefulness." Curr Opin Neurobiol **44**: 222-227.

Singer, S. J. (1975). "Membrane fluidity and cellular functions." Adv Exp Med Biol **62**: 181-192.

Takata, N. and H. Hirase (2008). "Cortical layer 1 and layer 2/3 astrocytes exhibit distinct calcium dynamics in vivo." PloS one **3**(6): e2525.

Tang, X., et al. (2009). "Heterogeneity of Kir4.1 channel expression in glia revealed by mouse transgenesis." Glia **57**(16): 1706-1715.

Tobaldini, E., et al. (2017). "Sleep, sleep deprivation, autonomic nervous system and cardiovascular diseases." Neurosci Biobehav Rev **74**(Pt B): 321-329.

Tononi, G. and C. Cirelli (2001). "Modulation of brain gene expression during sleep and wakefulness: a review of recent findings." Neuropsychopharmacology **25**(5 Suppl): S28-35.

Tononi, G. and C. Cirelli (2006). "Sleep function and synaptic homeostasis." Sleep Med Rev **10**(1): 49-62.

Verkhratsky, A. and M. Nedergaard (2018). "Physiology of Astroglia." Physiol Rev **98**(1): 239-389.

Vincent, A. M., et al. (2013). "Biology of diabetic neuropathy." Handb Clin Neurol **115**: 591-606.

Wang, X., et al. (2011). "ER stress modulates cellular metabolism." Biochem J **435**(1): 285-296.

Wu, M. M., et al. (2006). "Ca2+ store depletion causes STIM1 to accumulate in ER regions closely associated with the plasma membrane." J Cell Biol **174**(6): 803-813.

Yaffe, Y., et al. (2015). "The myelin proteolipid plasmolipin forms oligomers and induces liquid-ordered membranes in the Golgi complex." J Cell Sci **128**(13): 2293-2302.

Yoshikawa, F., et al. (2008). "Opalin, a transmembrane sialylglycoprotein located in the central nervous system myelin paranodal loop membrane." J Biol Chem **283**(30): 20830-20840.

Yousuf, M. S., et al. (2020). "Endoplasmic reticulum-mitochondria interplay in chronic pain: The calcium connection." Mol Pain **16**: 1744806920946889.

Zuber, B., et al. (2005). "The mammalian central nervous synaptic cleft contains a high density of periodically organized complexes." Proc Natl Acad Sci U S A **102**(52): 19192-19197.